MODELING ACOUSTIC BACKSCATTER FROM THE SEAFLOOR BY LONG-RANGE SIDE-SCAN SONAR

A Thesis

by

ANTHONY P. LYONS

Submitted to the Office of Graduate Studies of
Texas A&M University
in partial fulfillment of the requirements for the degree of

MASTER OF SCIENCE

December 1991

Major Subject: Oceanography

MODELING ACOUSTIC BACKSCATTER FROM THE SEAFLOOR BY LONG-RANGE SIDE-SCAN SONAR

A Thesis

by

ANTHONY P. LYONS

Submitted to the Office of Graduate Studies of
Texas A&M University
in partial fulfillment of the requirements for the degree of

MASTER OF SCIENCE

December 1991

Major Subject: Oceanography

MODELING ACOUSTIC BACKSCATTER FROM THE SEAFLOOR BY LONG-RANGE SIDE-SCAN SONAR

A Thesis

by

ANTHONY P. LYONS

Approved as to style and content by:

Aubrey L. Anderson
(Chair of Committee)

Robert O. Reid
(Member)

E. Fry /RA
Edward S. Fry
(Member)

Gilbert T. Rowe
(Head of Department)

December 1991

ABSTRACT

Modeling Acoustic Backscatter from the Seafloor

by Long-Range Side-Scan Sonar. (December 1991)

Anthony P. Lyons, B.S., Henderson State University

Chair of Advisory Committee: Dr. Aubrey L. Anderson

An existing model of seafloor backscattering [*Jackson et al.*, 1986a] was extended to include volume scattering from a random inhomogeneous continuum and scattering from subbottom interfaces. Results of computer simulations with the extended model were compared with values of scattering strength obtained from processed GLORIA data from the Monterey Fan off the coast of California. Regions of well delineated high and low backscatter are seen in the GLORIA imagery. The geoacoustic input parameters for the simulation runs were either taken directly from or estimated from core data obtained by ground truth sampling in the image area. From the model simulation results it was found that the low backscatter region is dominated by interface scattering from a single subbottom interface over a thick homogeneous sand layer. The high return regions are dominated by scattering from the random inhomogeneous continuum. The two additions to the scattering model have allowed the use of the ground truth measurements to constrain the input parameter values. No free parameters are required to fit the scattering strength data.

ACKNOWLEDGMENTS

I am deeply grateful for the patient instruction and guidance given me by my committee chairman, Dr. Aubrey L. Anderson. I would like to thank him for always making time for discussion throughout the progress of my research and for introducing me to the exciting world of Acoustical Oceanography. I thank my commitee members, Professor Robert O. Reid and Dr. Edward L. Fry, for their thoughtful suggestions regarding my thesis.

Many thanks to Dr. Fa S. Dwan for providing the GLORIA inversion data and for interesting discussions on our work. I am grateful to Dr. James V. Gardner and the United States Geological Survey for providing the ground truth data, which was a very large part of my research, and for providing the GLORIA image used in this thesis. The Naval Research Labs provided funding for this project; thank you NRL and Dr. David L. Bradley.

Thank you Kirt and Bill, my 304 Kyle family; without you it wouldn't have been as much fun (although I might have finished sooner). Thanks also to my many friends: Ricardo, Alex, Martin, Matt, George, Michelle, Mark, Greg, Steve, and the rest of the Oceanography group. Finally I must give my greatest thanks to my family for their love, encouragement, and constant interest in my education.

TABLE OF CONTENTS

LIST OF TABLES

LIST OF FIGURES

INTRODUCTION

General Introduction

Backscattering of sound from the seafloor is fundamental to the operation of many underwater acoustic systems. This is especially true for remote characterization of the ocean bottom with calibrated long-range side-scan sonar systems, such as the GLORIA (Geological LOng Range Inclined Asdic) system [*Mitchell and Somers*, 1989]. With the growing availability of long-range side-scan sonar data, it is becoming increasingly important to understand the seafloor characteristics and mechanisms that control backscatter.

Non-specular backscattering from the ocean bottom is generally considered to consist of two principal components: (1) backscatter at the water-sediment interface due to surface roughness and (2) scattering from inhomogeneities within the sediment volume. Backscattering at the water-sediment interface, particularly for sandy bottoms, is caused by surface roughness [*Boehme and Chotiros*, 1988]. This roughness is due to the individual sand particles; sand ripples; dunes which are primarily hydrodynamic in origin; and features resulting from bioturbation by marine animals. Inhomogeneities within the sediment can include buried rocks, shells or other debris, gas bubbles, microlayering, and marine organisms or their burrows within the

This thesis follows the style of the *Journal of Geophysical Research*.

sediment. A considerable amount of work has been reported concerning acoustic scattering from rough surfaces but only limited results are available from studies of scattering from within the sediment volume. A review and pertinent references are provided below.

Although numerous investigations of bottom backscattering have been reported (summaries and additional references of which can be found in *Urick* [1983], *Wong and Chesterman* [1968], and *Jackson et al.* [1986a]), the geoacoustic controls of the various scattering mechanisms in seafloor sediment are not well understood. Such an understanding is essential for developing acoustic remote sensing techniques and for constructing predictive models for bottom backscattering. Backscatter measurements in conjunction with measurements of the physical properties of the seabed are needed [*Jackson et al.*, 1986b]. The research described here addresses the physical mechanisms responsible for backscattering and their relative importance.

The work reported in this thesis was prompted by two studies in the same area of interest. From the work of another student, Shufa Dwan, estimates of backscattering strength from the geographical region of interest have been made by inverting GLORIA imagery data. Also, ground truth cores have been taken in the study region by the United States Geological Survey. These two studies are important because they provide *simultaneous* acoustical and geoacoustical data with the necessary detail for the same location. This allows testing of any model which is developed to address scattering mechanisms and geoacoustic controls that have previously been "free" parameters. The work presented in this study will serve as a

link between the geoacoustic parameters of the seafloor and the acoustic response of this seafloor as measured by a long-range side-scan sonar.

Side-Scan Sonar Scattering Physics

The fundamental purpose of long range side-scan sonar is to provide acoustic imagery of the seafloor. *Johnson and Helferty* [1990] give a good review of the basic concepts of side-scan sonar and the relationship of backscattering to the operation of the sonar. The side-scan receiver detects acoustic energy that is backscattered from the ocean bottom. This differs from radar images which are produced from radar energy which reflects from large-scale planar surfaces. With acoustic side-scan systems, little energy is returned by direct reflection; reflection is in the specular direction, away from the receiving transducers. Substantial acoustic energy will be backscattered to the receiver only by those areas of the seafloor that have both (1) a bottom roughness of the appropriate scale and (2) an acoustic impedance (defined as the product of density and sound velocity) significantly different from seawater.

The amount of energy backscattered by the seafloor also varies with the angle of incidence (or grazing angle) between the sound waves and the seafloor (which also depends on the slope of the bottom). There are several different scales of bottom topography which are important in the scattering process. The most important of these scales are: the regional slope, which is generally much larger than the acoustic wavelength, and the microtopography (or surface roughness), which is much smaller

than a wavelength [*Jackson et al.*, 1986a]. *Urick* [1983] provides a useful description of the interaction of sound with the seafloor.

Reflection of sound from the ocean bottom is easily understood but is not the dominant process in returning energy to side-scan systems. In fact if the seafloor were entirely flat then no energy would be returned to the transducers except that traveling a vertical path as with a depth sounder. Because the ocean bottom is rarely flat on the smallest scales, several processes will cause scattering in nonspecular directions including the direction of the receiving transducer. The small-scale roughness of the bottom will, by diffraction [*Felsen*, 1964], reradiate (scatter) some of the incident sound. This diffraction of the acoustic waves by features that are small compared to the wavelength will cause a measurable backscattered signal. When there is little penetration of sound into the seafloor, this interface roughness scattering is usually the major source of backscatter. In general, a rougher surface will show a higher value of backscatter than a smoother one with the same impedance values.

For low acoustic frequencies and in regions where there can be substantial bottom penetration, such as deep sediment layers, scattering by inhomogeneities within the volume of the sediment can contribute significantly to the backscatter. This internal volume backscattering can be larger than the scattering component from the interface roughness [*Crowther*, 1983; *Jackson et al.*, 1986a; *Stanton*, 1984]. The depth of acoustic penetration, and therefore the amount of subsurface scatterers involved in the reradiation of acoustic energy, depends on the frequency of the sound and the physical properties of the sediments. *Hamilton* [1980] has found that the acoustic attenuation in natural sediments generally increases linearly with frequency (the

details of this frequency dependence have been refined by *Stoll* [1985]). At frequencies less than about 10 kHz, the attenuation coefficient in the bottom is typically so low that energy can penetrate to significant depths and the backscattered field may be dominated by scattering from inhomogeneities within the sediment. Therefore low-frequency acoustic side-scan data contain more, or at least different, information about the properties of the seafloor than those obtained from high-frequency systems [*Johnson and Helferty*, 1990].

Background and Literature Review

Several seafloor backscattering models have been developed in order to include the underlying physics of the scattering mechanisms and to examine the relative importance of the individual parameters affecting the strength of the backscattered signal [*Crowther*, 1983; *Jackson et al.*, 1986a; *Stockhausen*, 1963]. In general, the goal of bottom backscattering measurements and subsequent data analysis has been to accurately relate bottom scattering strength to a small number of readily measurable bottom characteristics (see for example *Mourad and Jackson* [1989]). These efforts have included several theoretical approaches.

There are two well-known theoretical methods for calculating acoustic scattering from rough surfaces. One is based on the small roughness perturbation approximation [*Thorsos and Jackson*, 1989], which is also known as the Rayleigh-Rice approximation. The other is based on the Kirchhoff (or physical optics) approximation [*Thorsos*, 1988]. The Kirchhoff approximation requires that the scattering interface be relatively

smooth in the sense that the smallest radii of curvature of surface roughness features can be only slightly smaller than the acoustic wavelength [*Jackson et al.*, 1986a]. A model based on this approximation is described by *Clay and Medwin* [1977] and has been applied to bottom remote sensing by *Stanton* [1984]. The small-roughness approximation is valid for small radii of curvature, provided the interface relief is much smaller than the acoustic wavelength. The two-fluid perturbation approximation was applied to bistatic bottom scattering by *Kuo* [1964].

Stockhausen [1963] developed a flat-interface volume scattering model that includes refraction at the interface (with consequent critical angle effects) and attenuation in a statistically homogeneous sediment. *Crowther* [1983] combined Kuo's model for roughness scattering with a volume scattering model for a flat, refracting interface. He compares this model with experimental scattering of sound from sediment grains conducted by *Nolle et al.* [1963]. Stockhausen does not include any physical scattering mechanisms in his model but represents all possible processes by a single generic volume scattering cross section.

Modeling of ocean surface scattering has received more attention than bottom scattering and has exploited results from electromagnetic scattering theory. One model, which avoids many of the shortcomings of the Kirchhoff and Rayleigh-Rice approximations, combines the two and treats the topography as the sum of small- and large-scale surfaces. The large-scale surfaces must have radii of curvature comparable to or larger than the acoustic wavelength, and the small-scale surface must have relief small compared to a wavelength [*Jackson et al.*, 1986a]. *McDaniel and Gorman* [1982] show how this composite roughness model is applied to the sea surface. *Jackson et*

al. [1986a] and *Mourad and Jackson* [1989] apply the composite roughness model to the interface scattering component of seafloor backscattering. These last authors combine the interface scattering model with Stockhausen's volume scattering model and compare the results to several seafloor backscattering data sets. Their results indicate relatively good comparisons between model computations and data. A major component that is missing from their model, however, is the relationship between the sediment properties and the model's volume scattering "free parameters," such as the scattering cross section per unit volume.

This scattering cross section per unit volume, which is the "free parameter" in many volume scattering models, has been represented in several ways. One of the simplest is to model the sediment volume as a collection of spherical (Rayleigh) scatterers embedded in a homogeneous substance. The scattering function for a small nonresonant sphere was described by *Rayleigh* [1945]. A different approach is to model the sediment volume as a random inhomogeneous continuum. *Chernov* [1960] uses the continuum model to derive a scattering cross section for the ocean, while *Nassiri and Hill* [1986] use it to model ultrasonic scatter from human tissue.

The classical treatment of backscattering assumes that the signal is returned from a number of point scatterers. The contribution of each scatterer to the total backscattered power is then assumed to add incoherently [*Wyber*, 1985]. This allows the effect of the backscattering to be modeled by simply determining a backscattering coefficient per unit area or per unit volume (scattering cross section). This unit area or volume is defined to be a finite patch of the surface (or volume) large enough to embody the essential statistical properties of the entire surface (volume). The

scattering cross section, expressed in decibels, is referred to as the scattering strength. Expressing the scattering in terms of a cross section allows the interface scattering cross section and the volume scattering cross section to be combined in order to obtain a value for the total scattering strength (as in *Jackson et al.* [1986a] and *Mourad and Jackson* [1989]).

Field Data

Study Area

The study site chosen for the backscatter simulations is in the "Fingers Area" of the Monterey Fan off Southern California. This name was given to the area by U. S. Geological Survey scientists [*Gardner et al.*, 1991] because of the interfingering of light and dark regions (high and low backscatter return regions) in the GLORIA image of the area. The Fingers Area can be seen in the lower right hand corner of Figure 1. These contrasting light and dark regions are not the result of bathymetry as this area is flat. The Fingers Area has less than 5 m of relief and a gradient less than 1 : 600 [*Gardner et al.*, 1991]. The Fingers Area was chosen as the site of the present study primarily because estimates of backscattering strength versus grazing angle have been made for the area. These backscattering strength estimates were produced by inversion of GLORIA imagery data [*Dwan*, 1991] The site has also been extensively surveyed by the USGS and these ground truth data were obtained for the present study in the form of core data (grain size, density, and sound speed, as

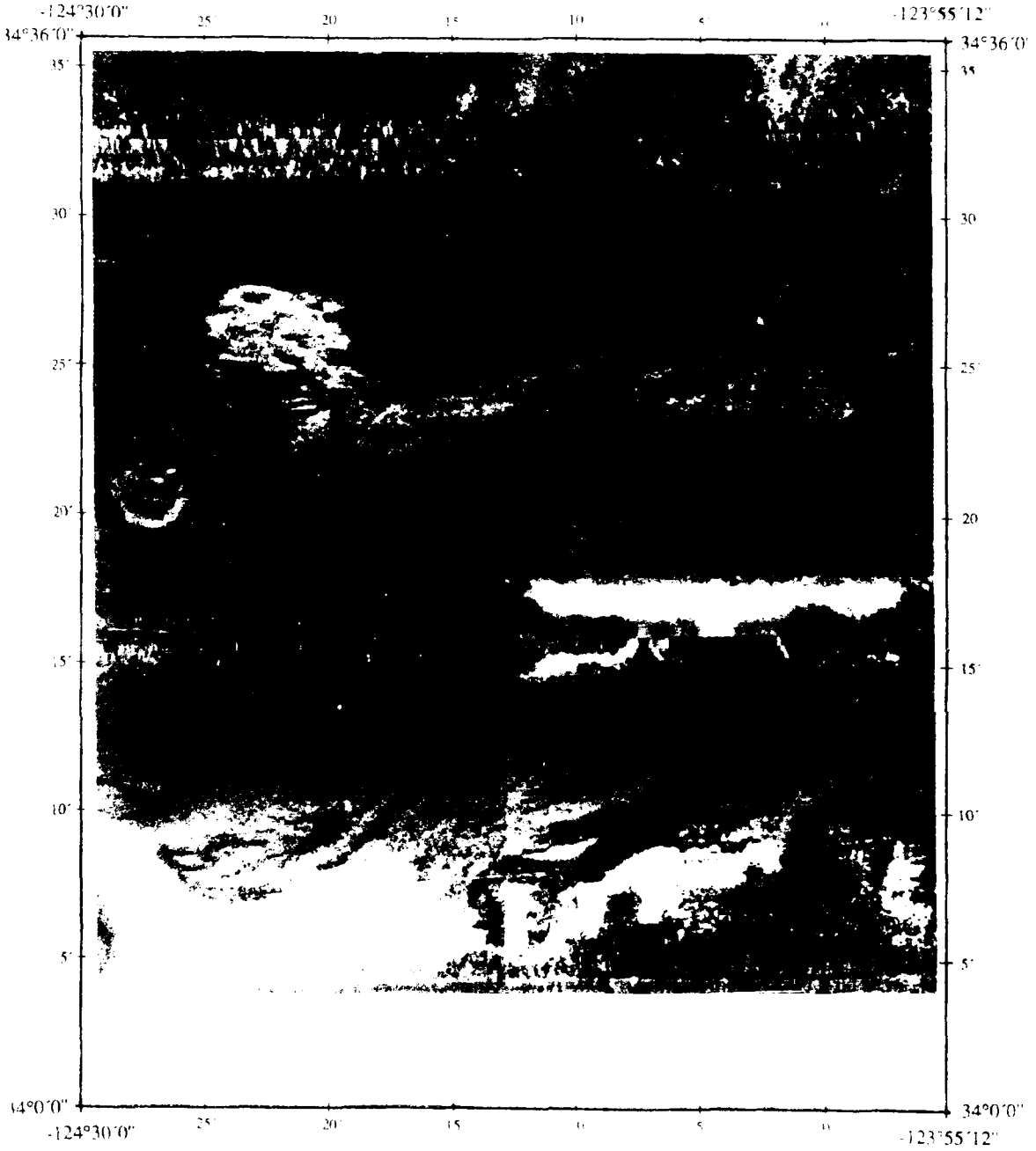

Figure 1. GLORIA image of study area.

seen in Figure 2 and Figure 3). The large, well-delineated contrast in the high and low backscatter return regions of the study site is advantageous in that it allows a separation of the different backscattering mechanisms that dominate in the high and low return regions.

The study area for this thesis lies at the edge of a distal depositional lobe of the Monterey Fan off south central California (Figure 4). The specific site is approximately 1000 km^2 in area and is uniformly of 4450 m water depth. A description of the region of ground truth measurements is provided by *Gardner et al.* [1991]. The study area is located on the eastern edge of what has been interpreted as the most recent depositional area of coarse-grained sediment. The depositional area has been covered by sediment deposited by turbidity currents that have traversed the length of Monterey Canyon, some 400 km in total length. The pathways provided by the bathymetric gradient funnel turbidity currents around and between two relatively large seamounts, although well-defined channels are not apparent. A GLORIA image (Figure 1) of the sediment depositional area clearly shows a high-backscatter pattern interlaced with a network of low-backscatter that resembles a braided-channel system [*Gardner et al.*, 1991].

Description of Relevant Bottom Properties

In the model used and extended for this research, the sediment is idealized as an acoustically refractive and lossy fluid, homogeneous except for small-scale variations in sound speed and mass density responsible for volume scattering. Gradients on scales of meters or less may be important in some cases, but are not included here. For

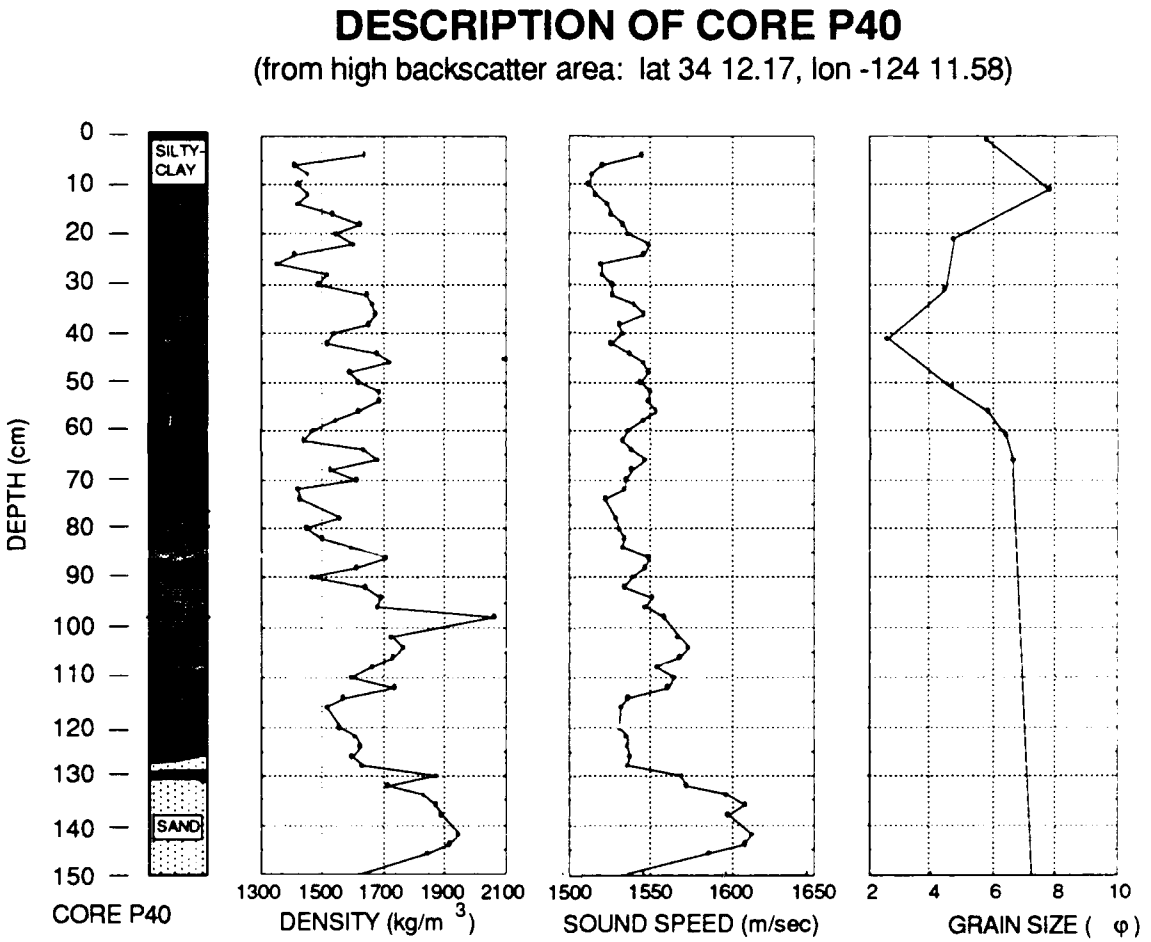

Figure 2. Example of ground truth data from high backscatter region.

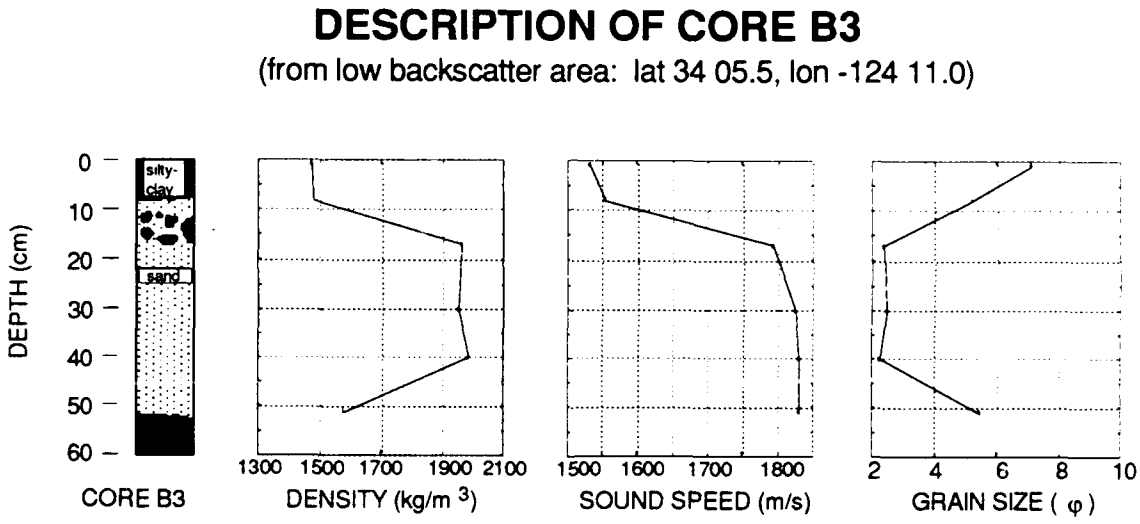

Figure 3. Example of ground truth data from low backscatter region.

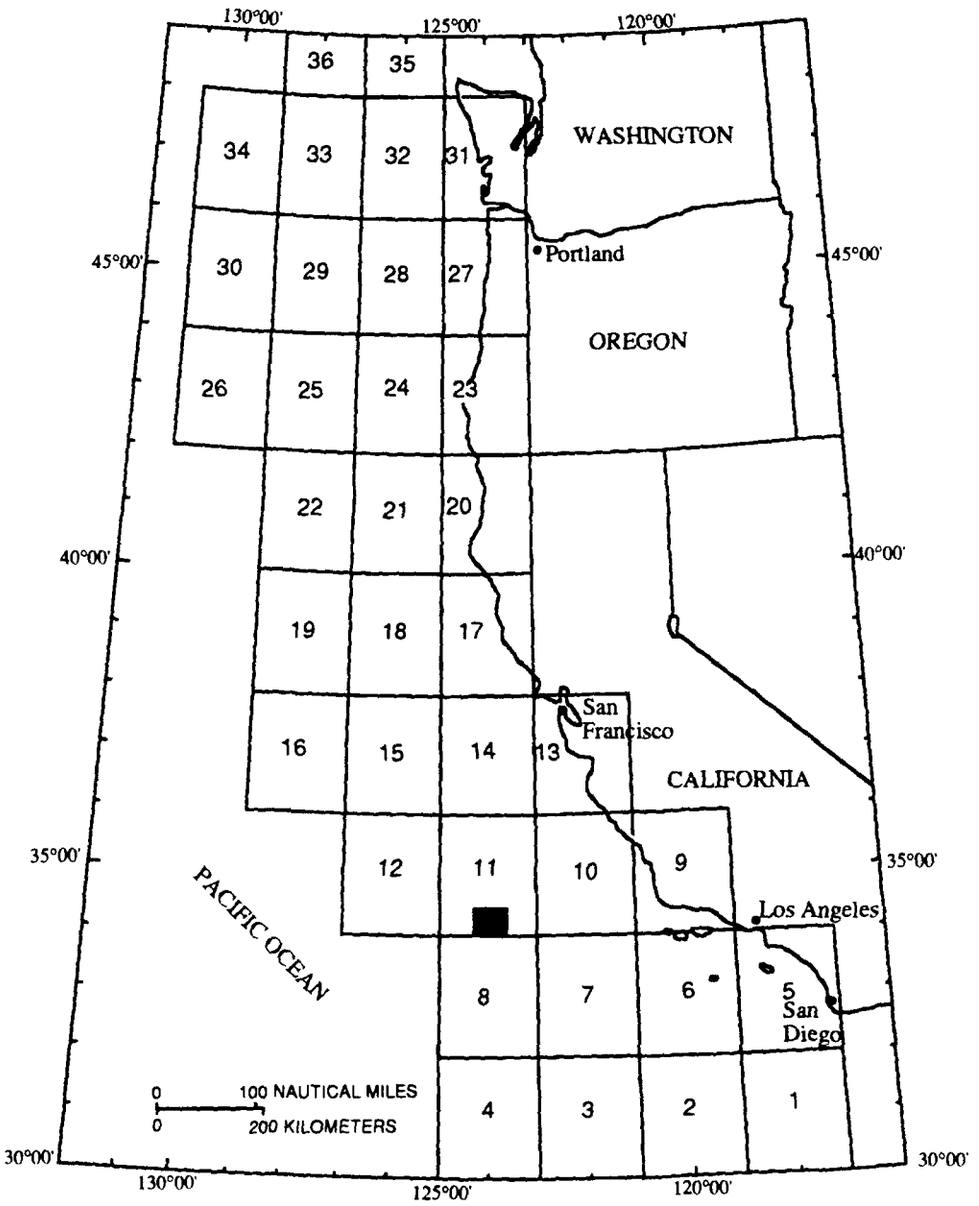

Figure 4. Study area (black rectangle at the bottom of region 11) .

such an idealized sediment, the volume parameters of interest are compressional wave attenuation, compressional wave speed, and mass density. The latter two parameters are used here to calculate volume scattering strength. Sediment attenuation loss is small and this is represented as an imaginary part of the wavenumber which is much smaller than the real part. *Hamilton* [1972], gives ratios of imaginary to real wavenumbers between 0.3 and 0.015. The relevant properties of the sediment can be broken up into two parts: those that are ascribed to the interfaces in the sediment and those ascribed to the volume between the interfaces. The properties of the volume will be discussed first and then the properties of the interfaces.

A good summary of data on compressional wave speed and mass density has been given by *Hamilton and Bachman* [1982]. Except for very high porosity surface sediments, the ratio of compressional wave speeds in the sediments to speed in the overlying water is usually somewhat greater than unity. Thus, acoustic energy transmitted from water to the sediment across the interface is refracted away from the normal. For grazing angles shallower than the "critical angle," at which the refracted ray becomes horizontal, penetration into a flat bottom will be negligible, and volume scattering should be unimportant. Very fine sediments, such as clay, may have speed ratios slightly less than unity, and may exhibit an angle of intromission rather than a critical angle when the bottom is flat. The mass density of sediments is typically between one and two times that of seawater. Mass density and compressional wave speed ratios are highly correlated. This high correlation allows some of the statistical properties of the sediment volume to be estimated with either the mass density or compressional wave speed.

Within the volume of the sediment (between interfaces) the properties are assumed to vary *continuously*. This continuous variation occurs as a small variation of the properties about their mean values (by contrast, an interface constitutes a discontinuity in the properties). For centimeter-length acoustic waves, it is likely that the most important inhomogeneity is not the graininess of the sediment, but larger-scale inhomogeneities. Therefore, instead of classifying the sediment according to type, the sediment must be classified in a more quantitative manner. The two parameters used to characterize the sediment volume are the correlation length (which gives an estimate of the size of the inhomogeneity) and the variance of density and of compressiblity.

In order to relate the compressibility, κ, (defined as $1/(\rho_0 c^2)$) or density, ρ, of one medium at one point to values in the same medium at surrounding points, one may introduce the correlation function, $N(r)$, of those variables as follows:

$$N_\kappa(r) = \frac{\langle \Delta\kappa_1 \Delta\kappa_2 \rangle}{\langle |\Delta\kappa|^2 \rangle}, \tag{1}$$

$$N_\rho(r) = \frac{\langle \Delta\rho_1 \Delta\rho_2 \rangle}{\langle |\Delta\rho|^2 \rangle}, \tag{2}$$

$$N_{\rho\kappa}(r) = \frac{\langle \Delta\rho_1 \Delta\kappa_2 \rangle}{(\langle |\Delta\rho|^2 \rangle \langle |\Delta\kappa|^2 \rangle)^{\frac{1}{2}}}, \tag{3}$$

Exponential and Gaussian forms for such correlation functions have been suggested by *Chernov* [1960] and *Ishimaru* [1978] in their studies of hydroacoustic transmission. *Crowther* [1983] used exponential correlation functions in the study of sediment volume backscattering. *Nicholas* [1976] and *Nassiri and Hill* [1986] used both

exponential and Gaussian models for the correlation function of soft biological tissues. In modeling the sediment volume, the assumption has been made that a single characteristic structure produces the dominant scattering effect at a given frequency. Thus the data have been analyzed in terms of a single correlation function. Based on the study of simultaneous variation of density and compressional wave speed in sediments [*Hamilton and Bachman*, 1982], it is assumed here that fluctuation of density and compressibility are inversely dependent (*i.e.* $N_{\rho\kappa}(r) = N_{\kappa\rho}(r) = -N(r)$, where $N(r)$ is the correlation function of variation of either density or compressibility). In this analysis the exponential correlation function will be used and is given as follows:

$$N(x) = exp(-x/d) \tag{4}$$

where d is the correlation length and x is lag in the generation of autocorrelation. The variance, cv, of compressibility and density is given as

$$cv = \left(\frac{\sqrt{\langle |\Delta\kappa|^2 \rangle}}{\kappa_0} + \frac{\sqrt{\langle |\Delta\rho|^2 \rangle}}{\rho_0} \right)^2. \tag{5}$$

Most data on interface roughness are derived from bathymetry having a resolution of 100 m or larger [*Fox and Hayes*, 1985]. One-dimensional spectra with centimeter-scale resolution presented by *Jackson et al.* [1986b] and *Fox and Hayes* [1985] agree with the lower resolution data in that both exhibit power-law roughness spectra. A good discussion and references on the statistics of power-law spectra is provided by *Jackson et al.* [1986a]. Random processes with true power-law spectra require careful treatment, as they are nonstationary and may not possess some of

the common statistical measures such as moments and correlation lengths. Such processes are special cases of *stationary increment* processes [*Jackson et al.*, 1986a]. In the present context, the random process of interest is the bottom profile $h(\mathbf{r})$, where $\mathbf{r}$ is the two-dimensional vector giving horizontal position. The term *stationary increment* implies that, while $h(\mathbf{r})$ may not be stationary, the random process defined as the difference $h(\mathbf{r}-\mathbf{r}_0)-h(\mathbf{r}_0)$ is stationary ($\mathbf{r}_0$ is an arbitrary horizontal displacement). In practical terms, this approach is useful when the relief has both small- and large-scale components, but the largest scales are well beyond the range of interest. For example, the largest scales may be geographic in size and of no interest in the high-frequency scattering problem. *Stanton* [1984] assumes that both the correlation length and rms surface height are small enough to be measured by lower frequency acoustics.

We will assume that the two-dimensional roughness statistics are Gaussian and isotropic with spectrum of the form

$$W(\mathbf{k}) = \beta k^{-\gamma}. \tag{6}$$

In this expression, $\mathbf{k}$ is a two-dimensional wave vector with magnitude equal to the wavenumber k, β is the spectral strength, and γ is the spectral exponent. *Briggs* [1989] and *Jackson et al.* [1986b] have found that the spectral exponent, γ, ranges from 3 to 3.5 in magnitude. The restriction to power-law spectra with isotropic statistics is made for simplicity and excludes, *e.g.*, bottoms with directional sand ripples.

The spectrum $W(\mathbf{k})$ is related to the structure function $D(\mathbf{r})$. The structure function is defined as the expected value of the square of the increment in $h(\mathbf{r})$ for fixed horizontal displacement:

$$D(\mathbf{r}) = E\{[h(\mathbf{r}+\mathbf{r}_0) - h(\mathbf{r}_0)]^2\}. \tag{7}$$

The spectrum and structure function are connected by the following transformation:

$$D(\mathbf{r}) = 2\int_{-\infty}^{+\infty}\int_{-\infty}^{+\infty}(1 - cos\mathbf{k}\cdot\mathbf{r})\,W(\mathbf{k})\,d^2k. \tag{8}$$

If the roughness statistics are isotropic the spectrum and the structure function will depend only on the magnitudes k and r of the two-dimensional vectors $\mathbf{k}$ and $\mathbf{r}$. The structure function corresponding to the isotropic spectrum of Eq. (6) is

$$D(\mathbf{r}) = C_h^2 r^{2\alpha}, \tag{9}$$

where

$$C_h^2 = [2\pi\beta\Gamma(2-\alpha)2^{-2\alpha}]/[\alpha(1-\alpha)\Gamma(1+\alpha)], \tag{10}$$

where Γ is the gamma-function and where

$$\alpha = (\gamma/2) - 1. \tag{11}$$

The integral in Eq. (8) is convergent for $0 < \alpha < 1$.

The structure function provides a measure of roughness that is easier to interpret, in some respects, than the power spectrum. Both the two-dimensional power

spectral density function and the structure function are used in the treatment of interface scattering.

Similarities between the descriptions of properties of the interfaces and the volume can be noted. The variance term of the volume description and the spectral strength, β, of the two-dimensional power spectral density each give a magnitude for the "roughness" of the ocean bottom. The correlation lengths of both the volume and interface descriptions give an average size of the scatterers involved. Values for all of the parameters described above were obtained from the USGS ground truth core data, either directly or indirectly, as will be discussed in the section on estimation of input parameters.

Inversion of GLORIA Data

The Fingers Area backscattering strength values used in the present study were inverted from GLORIA imagery. *Dwan* [1991] describes the steps taken to calculate backscattering strength values (BSS) by using the recorded GLORIA digital data from the Monterey Deep Sea Fan. The first step was to decode the recorded 8-bit compressed GLORIA data into 12-bit format. Then based on the transducer calibration value (pressure to voltage transfer function), the 12-bit values of data logger input voltage were mapped into a set of pseudo received acoustic pressure values in decibels (dB) relative to 1 $\mu V/\mu Pa$. The transducer calibration value represents the output voltage (in microvolts) at the transducer terminals resulting from an acoustic pressure of one micro-pascal on the transducer face for a plane wave arriving along the axis of the beam pattern. It is because the system gains are not

accounted for at this point that the pressure estimates are called "pseudo received levels." The second step was to remove the time varying gain of the system to recover the true relative acoustic pressure levels at the hydrophone face. Third, the processing gain and system gain were removed to recover the absolute received levels. Values resulting from application of these three steps to the recorded signals are estimates of the received levels (RL) at the hydrophone face.

Ray tracing techniques are used to account quantitatively for three factors that modify the sound pressure level as the side-scan pulse travels from source to receiver. These three factors are the effects of beam pattern (BP), transmission loss (TL) including both spreading loss and absorption, and the insonified area contribution (IA) for each sonar to seafloor eigen-ray. Because the GLORIA system beam pattern has not been measured, a calculated beam pattern was used for the data inversion. This beam pattern exhibits a null at nadir and a maximum of the main lobe at 40° to 45° off nadir. Uncertainty in this beam pattern restricts the data for useful backscattering strength estimates to those for rays with take-off angles which are removed a few degrees from this null direction. With values for the above described components, the seafloor backscattering strength can be calculated using an inverted form of the sonar equation:

$$BSS = SSP + BP + TL + IA + TL + BP - RL. \qquad (12)$$

where SSP is the sum of the source level, transducer calibration and logging calibration.

Backscattering strength values resulting from such an inversion of five pings of GLORIA data are shown versus grazing angle in Figure 5. With all of the system dependent factors, as well as the spreading geometry influences and seafloor area contribution removed from the original data that generated the GLORIA imagery, the resulting inverted values represent the quantitative acoustic response of the seafloor. On Figure 5 quantitatively correct values indicate the contrasting strong and weak return regions of the Fingers Area which were only qualitatively indicated in Figure 1.

Objectives

The objectives of this research include an assessment of the relative importance of different scattering mechanisms involved in seafloor backscattering of long range side-scan sonar signals and an incorporation of the results into improved modeling capability for seafloor backscattering calculation. The understanding resulting from such an assessment is necessary for the development of improved acoustic remote sensing techniques. Until the various bottom scattering mechanisms are understood, one cannot hope to quantify the observed grazing angle dependence or to take full advantage of the backscattering strength measurement as a remote sensing tool. The research requires physical modeling to understand which parameters control backscattering (grain size, porosity, roughness, etc.).

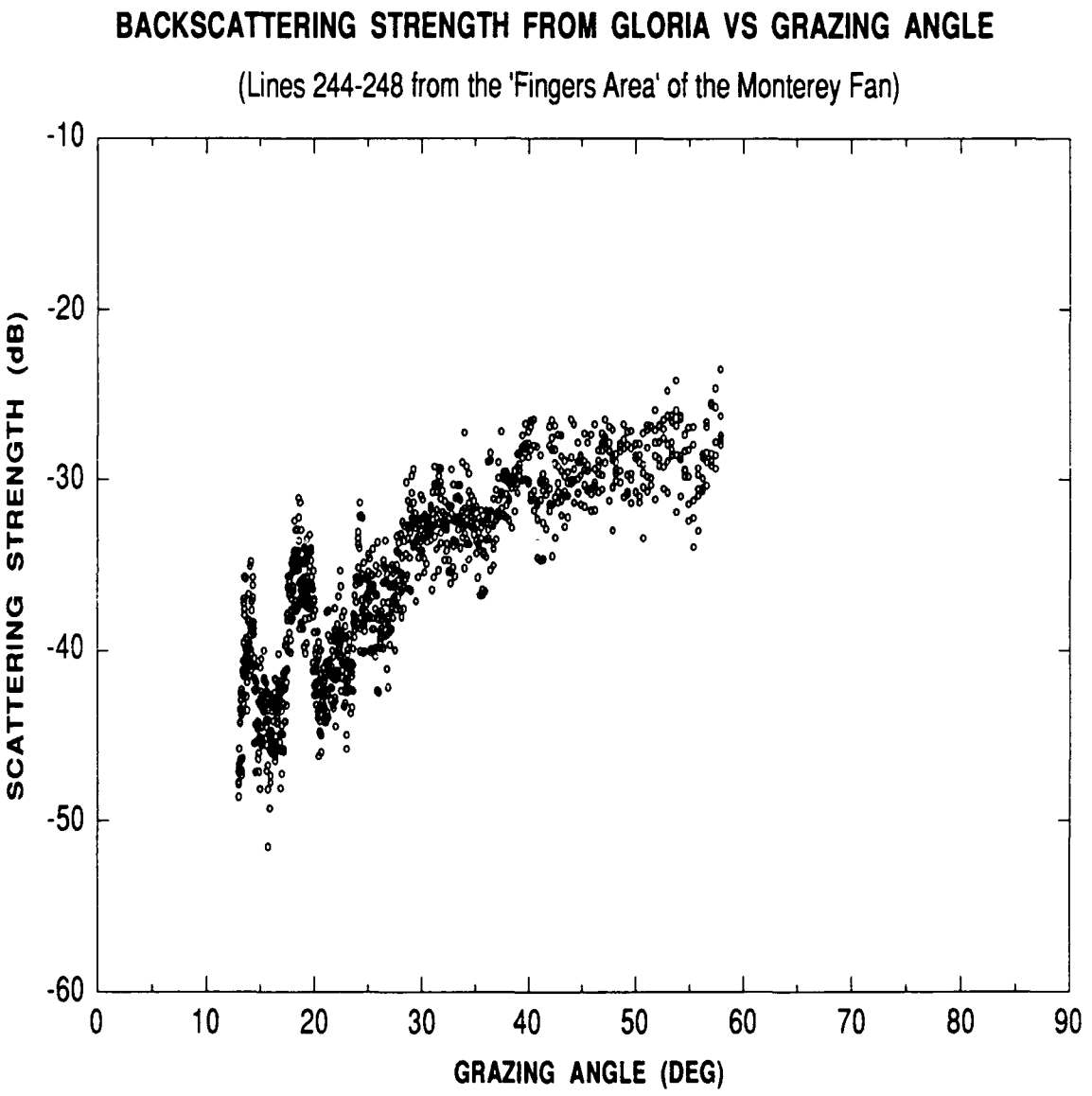

Figure 5. GLORIA inversion data.

The objectives of this work have been:

- To conduct an initial assessment of the comparison of predictions with existing seafloor backscattering models and measured data. The seafloor acoustic scattering model of *Jackson et al.* [1986a] was used with parameter estimates for the Monterey Fan area off the coast of California. These model predictions were compared with the backscattering values obtained by inversion of GLORIA data for the Fingers Area. The Monterey Fan parameters and GLORIA imagery were from the United States Geological Survey.

- To extend the model of *Jackson et al.* [1986a] by including specific volume scattering mechanisms such as subbottom interface scattering and scattering from an inhomogeneous continuum within the sediment. These additions to the model allow constraining values for the "free" parameter in the original model.

- To constrain all parameters used in the model simulations by information obtained directly or indirectly (such as with regression relations or from the literature) from ground truth cores in the study area. Results of constrained input model simulations are compared with data from the literature and with the inverted GLORIA data mentioned above.

- To use the results from addressing the first three objectives, together with sensitivity tests of the scattering model, in a quantitative evaluation of the relative importance of different mechanisms which contribute to backscattering from the seafloor of long range side-scan sonar energy.

METHODS

Introduction

The bottom backscattering strength model which was adapted for this study is based on the work of *Jackson et al.* [1986a]. This model assumes that the bottom material can be treated as a fluid and combines the composite roughness approximation, the Kirchhoff approximation, and a sediment volume scattering model to treat bottom backscattering at high frequencies. The composite roughness approximation includes the Rayleigh-Rice small-roughness perturbation approximation. Sediment sound absorption is included in the interface boundary condition. In this study, as in *Mourad and Jackson* [1989], some of the key integrals which occur in the scattering theory are numerically approximated by simple analytic expressions. The properties of the bottom material are assumed to be statistically homogeneous both vertically and horizontally in the model. Note that this does not mean that the properties are isotropic. The model includes microlayering by allowing a different value for correlation length in the horizontal than in the vertical.

The bottom backscattering strength, $S_b(\theta)$ as defined by *Urick* [1983] is the dB equivalent of the scattering cross-section, which we break into two parts:

$$S_b(\theta) = 10log_{10}[\sigma_i(\theta) + \sigma_v(\theta)], \tag{13}$$

where $\sigma_i(\theta)$ = the dimensionless backscattering cross-section per unit solid angle per unit area due to the water-sediment interface roughness and $\sigma_v(\theta)$ = the dimensionless backscattering cross-section per unit solid angle per unit volume due to scattering below the water-sediment interface. For the model developed in this study, the parameter $\sigma_v(\theta)$ can include scattering from one or more inhomogeneous continuums and/or scattering from one or more subbottom interfaces. A representation of the components of bottom backscattering is given in Figure 6.

Rayleigh-Rice Approximation

The composite roughness model applies the Rayleigh-Rice small-roughness perturbation approximation to the small-scale portion of the interface roughness spectrum. This approximation is valid if the small-scale rms relief is much smaller than the acoustic wavelength. The fact that one must consider the rms relief implies that the small-scale surface cannot have a power-law spectrum extending to arbitrarily low wavenumbers.

Most treatments of rough-surface perturbation theory assume an impenetrable boundary that is either a pressure release or a hard surface. For the penetrable, two-fluid interface, one must impose continuity of pressure and the normal component of velocity across the interface and then solve for the scattered field to first or second order in the relief $h(\mathbf{r})$. A first-order calculation is sufficient to obtain the expected value of the scattered intensity, from which the scattering cross section can

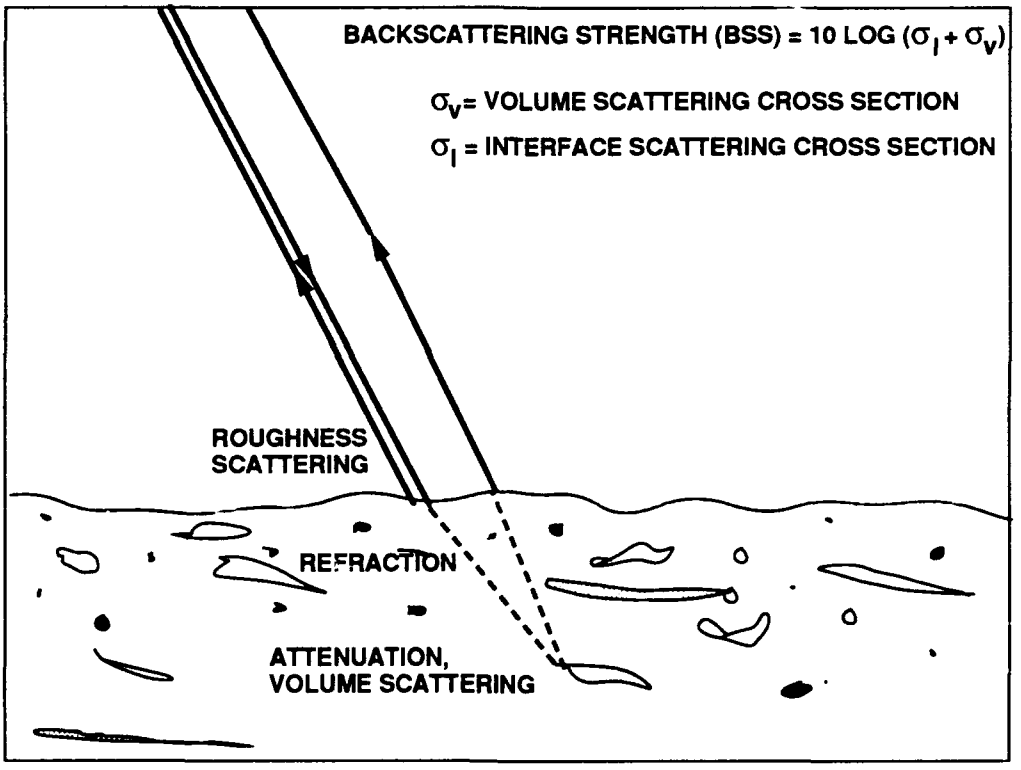

Figure 6. Representation of scattering.

be obtained. We will employ the backscattering cross section used by *Jackson et al.* [1986a] which was in turn obtained directly from *Kuo* [1964].

The sediment is taken to be a homogeneous fluid characterized by its mass density and compressional wave speed. Losses are neglected on the grounds that the imaginary part of the wavenumber is usually much smaller than the real part at the frequencies of interest. It is convenient to introduce the following ratios defining the essential sediment properties:

$$\nu = \frac{\nu_s}{\nu_w}, \tag{14}$$

$$\rho = \frac{\rho_s}{\rho_w}, \tag{15}$$

where ν_s, ρ_s are the sound speed and density on the sediment side of the water-sediment interface, and ν_w, ρ_w are the sound speed and density of the water. The small-scale backscattering cross section $\sigma_s(\theta)$ depends upon these quantities as well as upon the grazing angle θ and the acoustic wave number in water $k_a = \omega/\nu_w$. Assuming, without loss of generality, that the incident wave vector is parallel to the x-z plane and introducing the notation $W(k_x, k_y) = W(\mathbf{k})$, Kuo's cross section expression can be written (in the notation of Jackson *et al.*) as

$$\sigma_{rr}(\theta) = 4k_a^4 \sin^4\theta \, F(\theta, \nu, \rho) \, W(2k_a \cos\theta, 0). \tag{16}$$

This expression singles out a specific wavenumber in the two-dimensional roughness spectrum, the Bragg wavenumber $2k_a\cos\theta$. By using the term "Bragg wavenumber" it

is not implied that the rough surface must be periodic; it simply means that, out of the entire spectrum of interface wavelets, those having the Bragg wavenumber dominate backscattering when surface relief is much smaller than the acoustic wavelength. As long as the interface relief is small, Eq. (16) has a wide range of validity, including anisotropic and non-Gaussian interfaces, but we will consider the isotropic Gaussian case.

In this expression $F(\theta, \nu, \rho)$ is the complex function

$$F(\theta \quad, \rho) = \frac{(\rho - 1)^2 cos^2(\theta) + \rho^2 - k'^2}{[\rho\, sin(\theta) + P(\theta)]^2}, \tag{17}$$

where k' and $P(\theta)$ are

$$k' = \frac{k_2}{k_1} = \frac{k_{2r} + k_{2i}}{k_1} = \frac{1}{\nu}[1 + i\delta], \tag{18}$$

$$P(\theta) = \sqrt{k'^2 - cos^2(\theta)}, \tag{19}$$

where δ is the loss tangent (ratio of imaginary wavenumber to real wavenumber for the sediment). The range of validity for the Rayleigh-Rice approximation is discussed in detail by *Thorsos and Jackson* [1989].

Composite Roughness Model

McDaniel and Gorman [1983] give derivations and references for the composite roughness model for impenetrable surfaces. The approach used in the present study

is that of *Jackson et al.* [1986a]. In the composite roughness approximation, the small-roughness perturbation approximation is used with corrections for shadowing and large-scale bottom slope. The model assumes that backscattering is due to small-scale roughness, with local grazing angle dependent on the slope of the large-scale surface.

The composite roughness approximation uses the large-scale rms bottom slope, s, calculated by partitioning the roughness spectrum into large-scale and small-scale parts. The cutoff wavenumber marks the boundary between the two parts and must be chosen so that the small-scale surface satisfies the conditions for validity of the Rayleigh-Rice approximation. In addition, the cutoff must be chosen so that the large-scale surface can be treated as locally flat (but not necessarily horizontal). The condition on the small-scale surface will be taken to be $2kh < 1$ [*Jackson et al.*, 1986a]. The small-scale roughness and large-scale slope can be found in terms of the spectrum of surface relief (assuming isotropy). This result, together with the cutoff condition on the small scale surface, yields the following expression for the slope

$$s^2 = \frac{(2\pi\beta h_0^{-\gamma})^{\frac{1}{\alpha}}}{2(1-\alpha)} \left[\frac{k_a^2}{\alpha}\right]^{\frac{1-\alpha}{\alpha}}, \tag{20}$$

where h_0 is a reference length equal to 1 cm.

With the assumption that the slope of the large-scale surface is Gaussian-distributed, the backscattering cross section for grazing angles of about 70° or less is obtained by averaging the small-scale backscattering contributions over the large-scale bottom slopes, s_x, with rms slope equal to s. The resulting cross section expression is:

$$\sigma_{cr} = \frac{R(\theta, s)}{\pi^{1/2} s} \int_{-\theta}^{\infty} \sigma_{rr}(\theta + s_x) exp(-s_x^2 s^{-2})\, ds_x. \tag{21}$$

$R(\theta, s)$ accounts for shadowing by the large-scale surface and is given by *Wagner* [1967] as

$$R(\theta, s) = (2Q)^{-1}(1 - e^{-2Q}), \tag{22}$$

where

$$Q = (1/4t)[\pi^{1/2} e^{-t^2} - t(1 - erf\, t)], \tag{24}$$

$$t = s^{-1} tan(\theta), \tag{23}$$

with erf being the error function. The integral of Eq. (21) is approximated in this study by a three-point Gauss-Hermite quadrature.

Kirchhoff Approximation

The preceding discussion of the composite roughness model was based on the assumption that the grazing angle at which the acoustic field is incident on the seafloor is about 70° or less. At steeper angles, application of the composite roughness model is more complicated and open to question [*Jackson et al.*, 1986a]. Instead of using the composite roughness model at steep grazing angles, the Kirchhoff approximation is used. This is possible because the Kirchoff criterion is much less stringent at steep

grazing angles, making it unnecessary to subtract the short-wavelength portion of the interface before applying the Kirchhoff approximation.

Considering the definition of scattering strength (Eq. (13)), the scattered intensity is usually taken to be the incoherent intensity, defined as the total intensity minus the coherent intensity. The coherent intensity is defined as the square of the expected value of the scattered field. When the rough-surface relief is comparable to or greater than the acoustic wavelength, the coherent intensity is usually a negligible fraction of the total intensity. This is the situation of interest here.

In the Kirchhoff approximation, when the coherent intensity is negligible, the backscattering cross section is given by the expression

$$\sigma_k(\theta) = \frac{g^2(\pi/2)}{8\pi\, sin^2\theta\, cos^2\theta} \int_0^\infty exp(-qu^{2\alpha}) J_0(u) u\, du, \tag{25}$$

where

$$q = sin^2\theta\, cos^{-2\alpha}\theta\, C_h^2\, 2^{1-2\alpha}\, k_a^{2(1-\alpha)}, \tag{26}$$

and

$$g(\theta) = \frac{y-1}{y+1}, \tag{27}$$

with

$$y = \frac{\rho sin\theta}{P(\theta)}. \tag{28}$$

The parameter $g(\pi/2)$ is the plane-wave reflection coefficient for normal incidence with $P(\theta)$ given by Eq. (19), J_0 is the zeroth order Bessel function of the first kind, k_a is the acoustic wavenumber in the water, and C_h^2 and α are related to the roughness spectrum of the interface (see Eqs. (10) and (11)). An approximation of the integral in Eq. (25) is made [*Mourad and Jackson*, 1989] based upon special cases for which exact analytical evaluation is possible. The Kirchhoff integral can be evaluated analytically for a pressure-release surface for the special case $\alpha = 1/2$ and $\theta = \pi/2$. The first step in the evaluation is to assume that the backscattering cross-section for the fluid-fluid boundary for $\theta = \pi/2$ is given by the pressure release result multiplied by $|g(\pi/2)|^2$, the squared magnitude of the Rayleigh reflection coefficient for vertical incidence. Next, the algebraic form of the integral in Eq. (25) for the $\alpha = 1/2$ case is employed but generalized by introducing two free parameters, a and b. These parameters are fixed by requiring that the correct $\theta = \pi/2$ result is obtained and also by requiring that the estimated backscattered intensity for an omnidirectional *cw* transmission agree with the Kirchhoff prediction [*Mourad and Jackson*, 1989]. This gives a constraint on the integral of the backscattering cross-section over the area of the bottom. The resulting approximation of Eq. (25) is

$$\sigma_k(\theta) = \frac{bq_c|g(\pi/2)|^2}{\frac{8\pi[cos^{4\alpha}(\theta)+aq_c^2sin^4(\theta)]^{1+\alpha}}{2a}}, \tag{29}$$

where C_h^2 and α are from the structure function Eqs. (10) and (11), and where

$$a = \left[\frac{8\alpha^2\Gamma\left(\frac{1}{2\alpha}+\frac{1}{2}\right)}{\Gamma\left(\frac{1}{2}\right)\Gamma\left(\frac{1}{\alpha}\right)\Gamma\left(\frac{1}{2\alpha}\right)}\right]^{2\alpha}, \tag{30}$$

and

$$b = \frac{a^{\frac{1}{2}+\frac{1}{2\alpha}}\Gamma\left(\frac{1}{\alpha}\right)}{2\alpha}. \tag{31}$$

The range of validity of the Kirchhoff approximation is discussed by *Thorsos* [1988].

The composite roughness and Kirchoff cross-sections are combined via an interpolation scheme by *Mourad and Jackson* [1989]. The scheme is as follows:

$$\sigma_i(\theta) = f(x)\sigma_k(\theta) + [1 - f(x)]\sigma_{cr}(\theta) \tag{32}$$

where

$$f(x) = \frac{1}{1 + e^x}, \tag{33}$$

$$x = 80[cos(\theta) - cos(\theta_{kdB})], \tag{34}$$

$$cos(\theta_{kdB}) = \left(\frac{1}{C_4} + 4\right)^{-\frac{1}{4}}, \tag{35}$$

$$C_4 = (1000)^{\frac{1}{1+\alpha}}(a\,q^2)^{\frac{1}{\alpha}}. \tag{36}$$

With this interpolation, the total interface backscattering cross section, $\sigma_i(\theta)$, is dominated by the Kirchoff cross section for seafloor grazing angles from 90° down to the angle for which the Kirchhoff cross-section has fallen 15 dB below its peak

value at 90°. For lower grazing angles, $\sigma_i(\theta)$ is predominately determined by the composite roughness cross section term.

Subbottom Contributions

One shortcoming of many backscattering models is the use of a "free" parameter to represent all scattering mechanisms within the volume of the sediment (*i.e.* everything below the water-sediment interface). This volume scattering component is probably dominant at the GLORIA frequency of 6.5 kHz in soft sediments where the acoustic energy can penetrate to significant depth into the seafloor. One of the major goals of this study has been to develop and test a model for the volume portion of the backscattering wherein all parameters are constrained by information that could be obtained from ground truth data (*e.g.* cores). Guided by the core descriptions for samples from the Fingers Area, two possible sources of scattering beneath the water-sediment interface were identified. Subsequent improvements to the volume scattering model were generated to incorporate these scattering sources into the parameterizations of internal volume backscattering. These sources are: (1) scattering from subbottom interfaces and (2) scattering from the random inhomogeneous continuum of the volume.

Subbottom Interfaces

The descriptions of several seafloor cores from the Fingers Area suggest that, in this area, subbottom interfaces might be important contributors to acoustic scattering from the water-sediment interface. Core B3 (Figure 3), from the low backscatter

region, is an example of such a core. To model the influence of a subbottom interface, the computation of composite roughness cross section (Eq. (21)) and Kirchhoff cross section (Eq. (25)) are made for the subbottom interface as was done for the water-sediment interface. Included in these computations for the buried interface are the effects of transmission loss at the water-sediment interface, refraction and subsequent ray path lengthening (or shortening) between the two interfaces, and attenuation along this portion of the ray path. These effects and the estimates of values for parameters ρ, ν, δ, γ, and β for the subbottom interface are constrained by core information. A representation of the effects included by adding a subbottom interface is given by Figure 7.

Two-way transmission loss associated with energy transmitted across the water-sediment interface is given by

$$[1 - g^2(\theta)]^2, \tag{37}$$

where $g(\theta)$ is the plane wave reflection coefficient for the interface as given by Eq. (27). Ray path lengthening is calculated by dividing the depth, z, to the second interface by $sin(\theta_2)$, where θ_2 is the refracted angle given by

$$\theta_2 = sin^{-1}[1 - (\nu cos\theta)^2]^{1/2}. \tag{38}$$

If the ray path length to the subbottom interface is longer than the spatial pulse length $(\nu_s \tau/2)$,which is about 7 m for the GLORIA system, then the subbottom contribution is set to zero. τ, the effective pulse length, is equal to the inverse of the

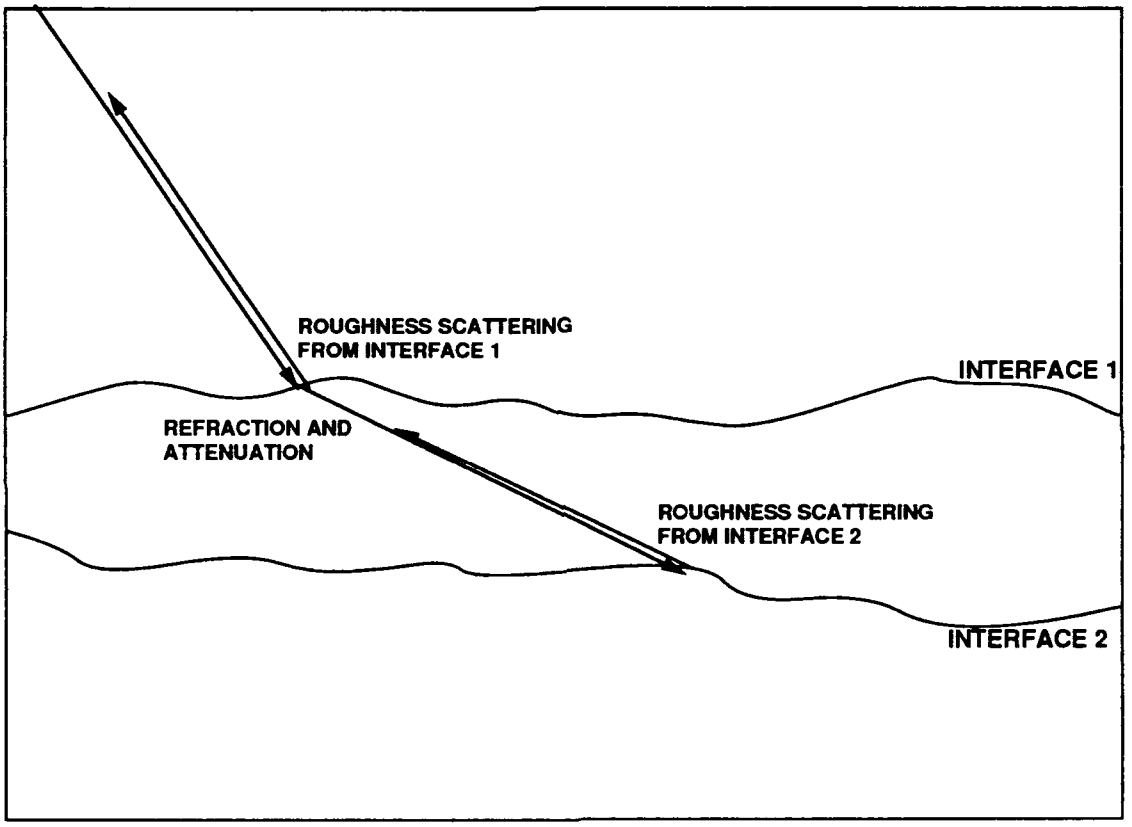

Figure 7. Representation of subbottom interface scattering.

bandwidth (100 Hz for the GLORIA system [*Chavez*, 1986]). Two way attenuation is given by

$$10^{-\frac{2\alpha_2 z}{10 sin\theta_2}}, \tag{39}$$

where α_2 is the attenuation coefficient discussed in *Hamilton* [1972] and calculated from the relation

$$\delta = \frac{k_{2i}}{k_{2r}} = \frac{\alpha_2 \nu \nu_w ln(10)}{f 40\pi}. \tag{40}$$

Inhomogeneous Continuum Scattering Model

One possible model for sediment volume scattering is that which consists of distributions of discrete random scatterers (Rayleigh scatterers). This model is appropriate when scatterers are well defined and scatter the wave noninteractively. In the sediment volume for some regions of the Fingers Area, the structure is very complicated (see for example Figure 2, a core from the high backscatter region). In such a sediment, separate "scatterers" and "homogeneous matrix" cannot be defined clearly. Thus a more realistic model for the sediment is that of an inhomogenous continuum. In this model, the acoustic properties of the sediment are assumed to fluctuate continuously, by a small amount, about their mean values. It is easier to obtain relevant volume parameters from such ground truth cores for an inhomogenous continuum model than for a discrete scatterer model. The inhomogeneous continuum model has been developed by *Chernov* [1960], *Nicholas* [1976], and *Nassiri and Hill* [1986]. Nicholas gives a complete derivation of the theory of scattering from a

random inhomogenous continuum. The expression for backscattering cross section per unit volume for an isotropic scattering inhomogeneous continuum, when the inhomogeneities are described by an exponential correlation function, is given as (following *Nassiri and Hill* [1986])

$$\mu = \frac{k^4 d^3}{2\pi}\left(\frac{\sqrt{\langle|\Delta\kappa|^2\rangle}}{\kappa_0} + \frac{\sqrt{\langle|\Delta\rho|^2\rangle}}{\rho_0}\right)^2 [1 + 4k^2d^2]^{-2}. \tag{41}$$

The two new parameters of interest are the correlation length, d, and the variance of compressibility and density, given by the $(\,)^2$ term. Figures 8 and 9 show the influence of these two parameters on the value of the backscattering cross section per unit volume. The scattering cross section is linearly dependent on the variance term (Figure 8). The correlation length dependence has a more complicated shape (Figure 9) with a scattering cross section peak at about 3 cm at $6.5kHz$. Thus, inhomogeneities with correlation length values around 3 cm will dominate the scattering at this frequency. This sensitive dependence of backscattering cross section on correlation length significantly influences the grazing angle dependence of scattering. Figure 10 shows how the interdependence shown in Figure 9 depends on frequency. The scattering cross section peak moves toward smaller correlation lengths and becomes more pronounced as frequency increases.

Anisotropy is included by considering the sediment to consist of a vertical stack of horizontal microlayers. Such a sediment model would have a finite correlation length in the vertical and an infinite correlation length in the horizontal. The increase of correlation length as grazing angle decreases is expressed as:

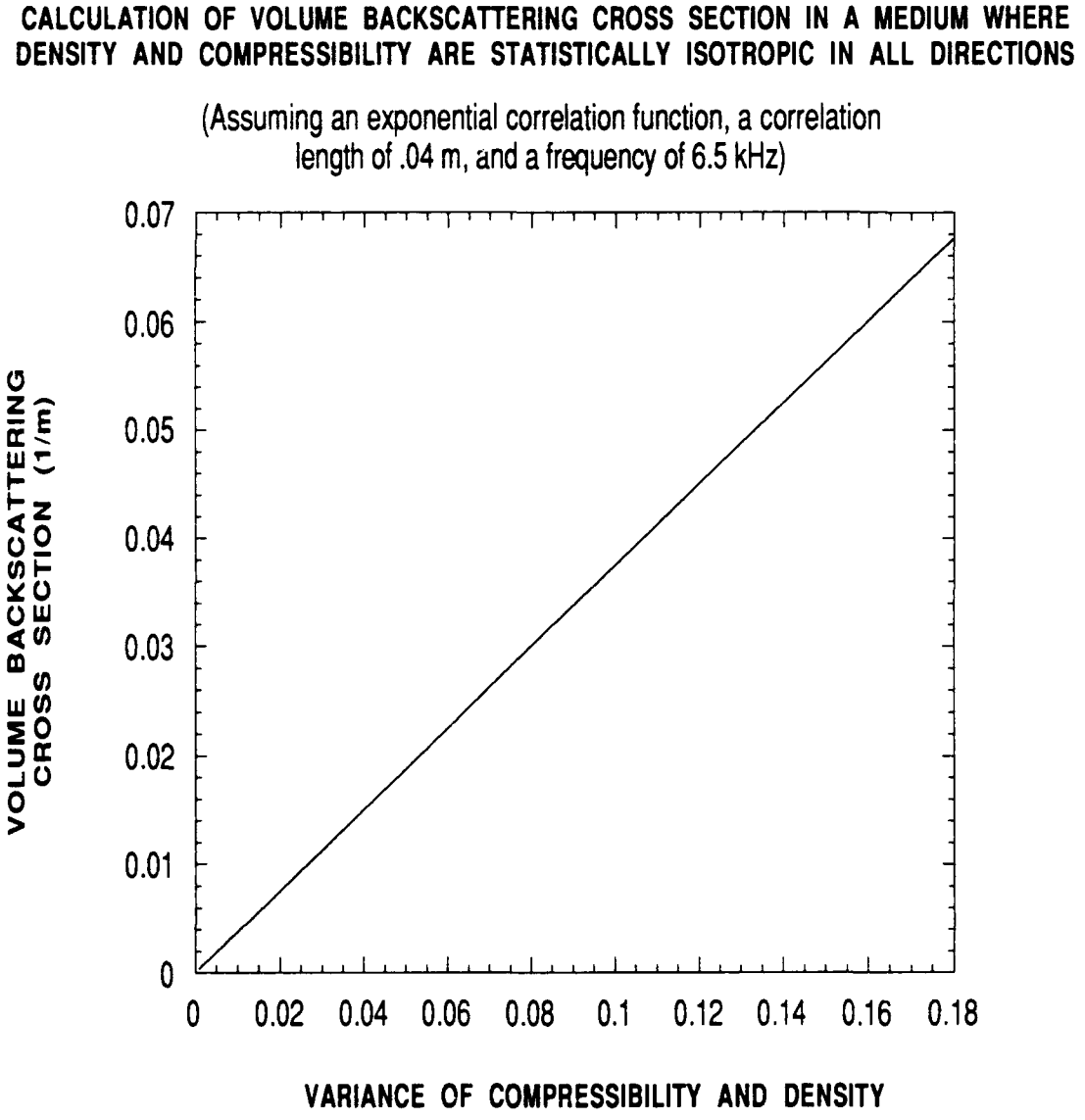

Figure 8. Volume scattering cross section as a function of variance.

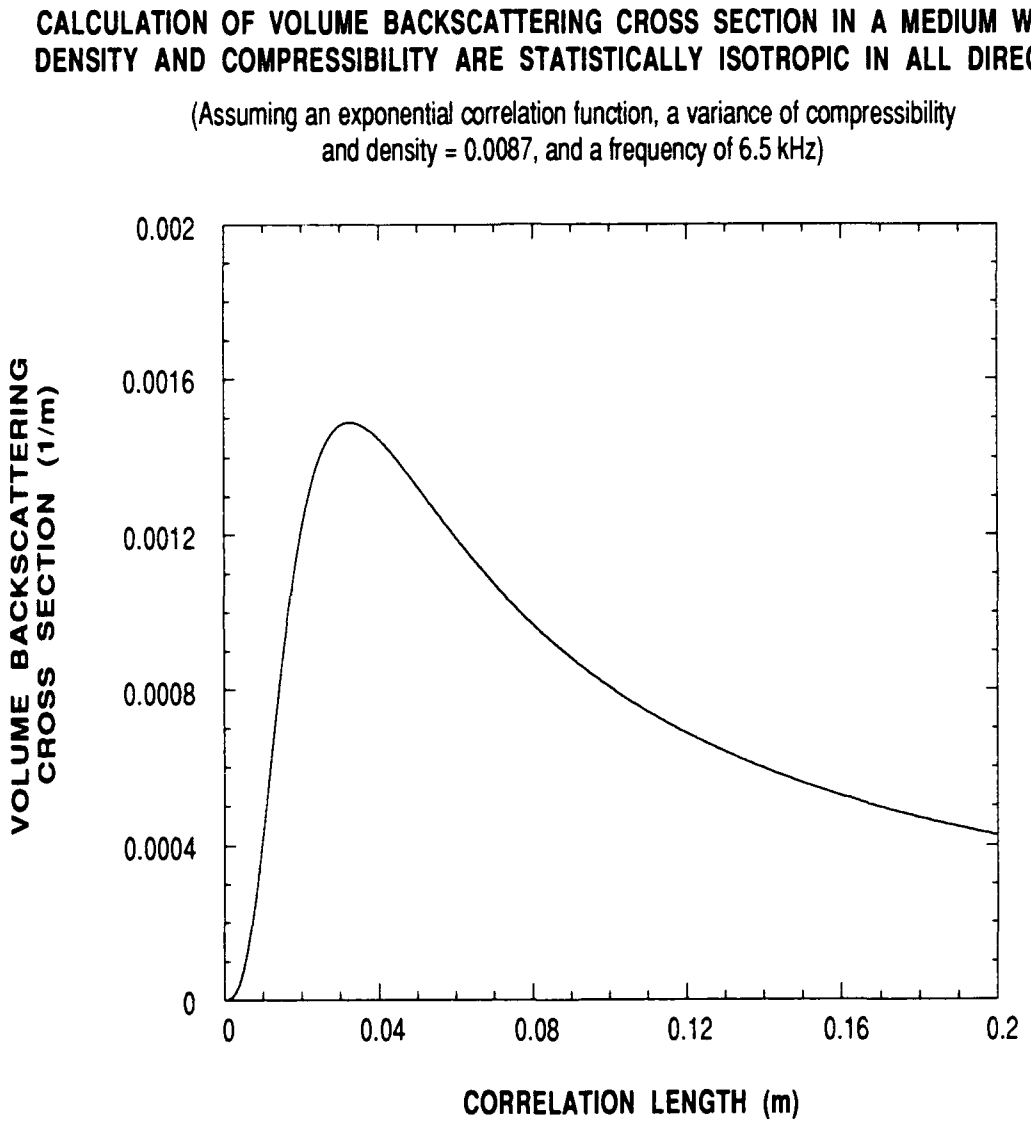

Figure 9. Volume scattering cross section as a function of correlation length.

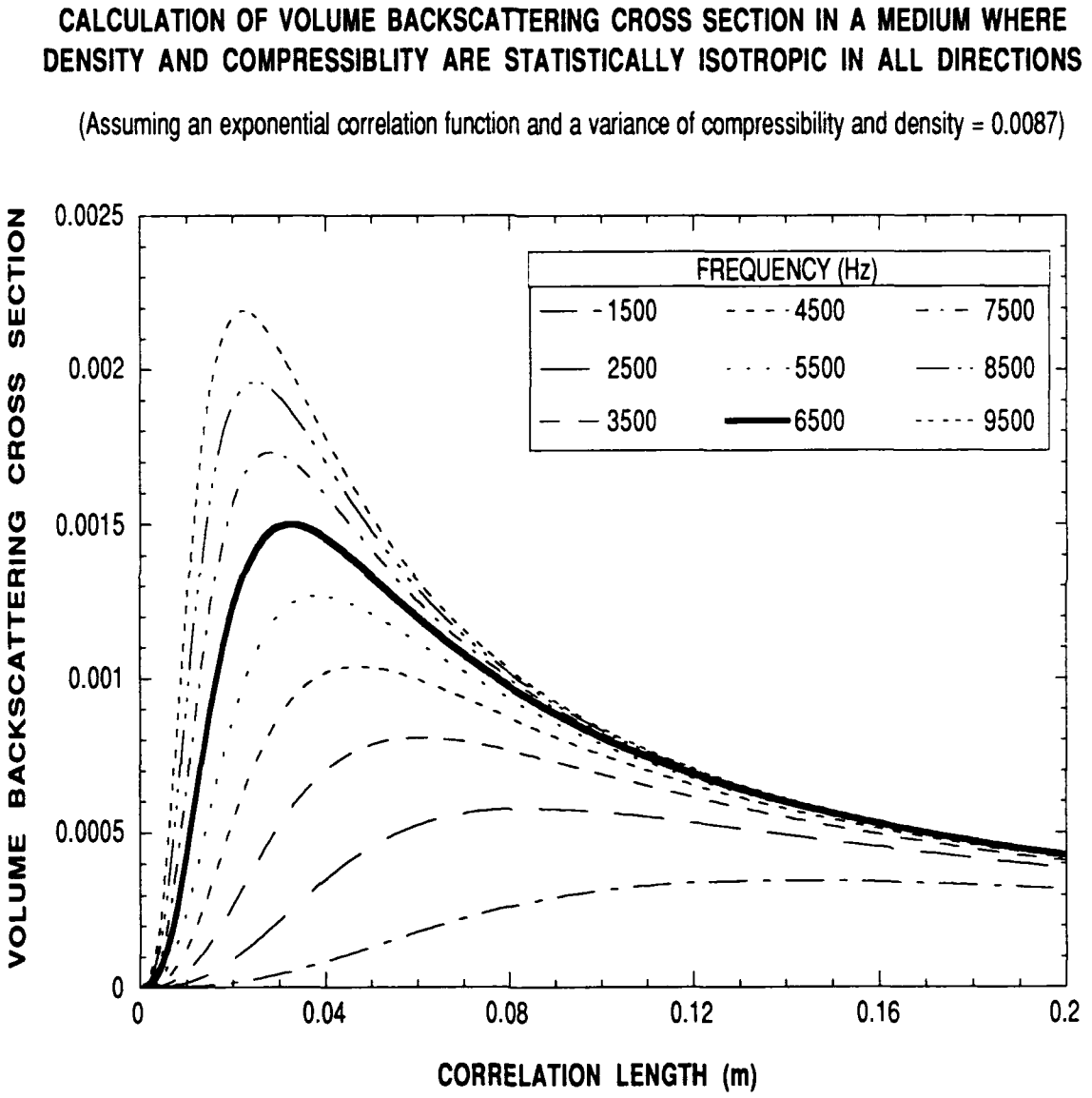

Figure 10. Frequency dependence of volume scattering cross section versus correlation length.

$$d' = d/sin(\theta_2). \tag{42}$$

See Figure 11 for the effect of this transformation on the volume scattering cross section versus grazing angle for a fixed vertical correlation length of 4 *cm* and variance of density and compressibility of 0.0087. In the absence of this transformation, *i.e.* the isotropic case, the volume scattering cross section would be a constant value for all grazing angles.

In the seafloor scattering model extension developed in the present study, the volume scattering cross section per unit volume; as obtained with Eq. (41), with or without anisotropy, is used in the model of *Stockhausen* [1963]. The Stockhausen model includes transmission loss, refraction and attenuation in a statistically homogenous sediment with a perfectly flat interface. The resulting expression includes the effect of absorption on the transmission coefficient of the sediment-water interface and on volume scattering. Bottom slope corrections and shadowing are taken into account in the same way as in the composite roughness model (Eq. (21)). The resulting equivalent surface scattering strength is written as

$$\sigma_v(\theta) = \frac{\mu[1 - g^2(\theta)]^2 sin^2(\theta)\,\alpha}{2\,sin(\theta_2)}. \tag{43}$$

The term α is the smaller of 1/attenuation, path length to the next interface, or spatial extent of acoustic pulse, where attenuation is given by

$$4\pi\mu + Im(k'). \tag{44}$$

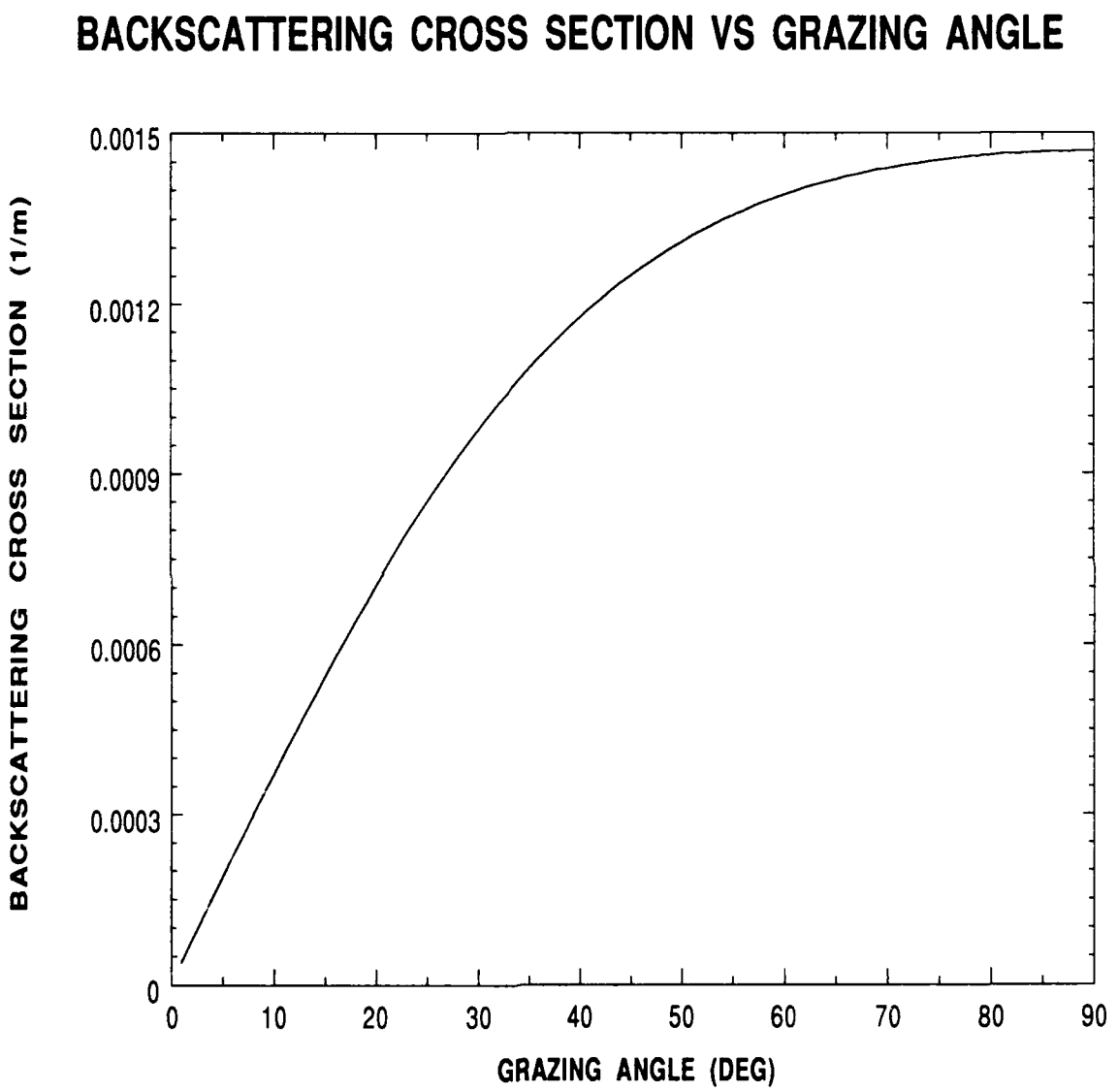

Figure 11. Effect of anisotropy on volume scattering cross section.

Eq. (44) includes attenuation by isotropic scattering and absorption and is valid in the single scattering regime. This is analogous to the first order perturbation regime for which the Rayleigh-Rice approximation is applicable. The dimensionless result of multiplying the backscattering cross-section, μ, by α is, in essence, a surface scattering parameterization of the volume scattering cross section of Eq. (41). The effects of additional inhomogeneous continuums at greater depths in the sediment can be added in the same manner as was the addition of subbottom interfaces.

The complete model for bottom backscattering cross section is now obtained by taking the sum of all the interface roughness and volume expressions. This approach has several inherent assumptions. It assumes, for example, that there are no correlations between the parts of the scattered field that result from interface roughness and those that result from volume inhomogeneities. Eq. (43) assumes that multiple scattering is negligible. This assumption implies that, of the energy incident upon each elemental volume, none (or a negligible amount) is from scattering by the rest of the sediment. The single scattering assumption is valid if attenuation in the sediment is due mostly to absorption. Since backscattering values from this study are found to be weak and attenuation due to absorption is about three orders of magnitude larger than attenuation due to scattering it may be assumed that each backscattered wave is composed of energy that has been scattered only once.

Related to the single-scattering assumption is the additional assumption that the influence of interface roughness on the acoustic field below is negligible. This is reasonable and is also inherent in the assumptions of the composite roughness model. The interface roughness only produces a small perturbation to the field.

Estimation of Input Parameters

The model discussed in the previous section relies on seven geoacoustic input parameters: the density ratio, ρ; sound speed ratio, ν; loss tangent, δ; correlation length of density or compressiblity variations, d; variance of density and compressibility, cv; spectral exponent, γ; and the spectral strength, β. One of the objectives of this thesis investigation was to fully constrain all of the parameters used in the model simulations by information obtained directly or indirectly (*i.e.* regression relations or other relationships from the literature) from ground truth cores in the study area. In this section the method for estimation of each of the seven model input parameters is discussed.

Ground truth information consisted of box core data and piston core data. The cores were sampled every 2 *cm* for values of density, sound speed, and grain size. Examples of the type of information obtained from cores are shown in the profiles of Figures 2 and 3.

Density and sound speed values were estimated for the interface by taking the average of values measured down to 22 *cm* (approximately one wavelength) below the interface. While this choice is rather arbitrary it is probably closely related to what the acoustic field "sees" as the interface. The fluctuations of density and sound speed are also small, so the values produced by averaging over other similar depth intervals will not differ significantly from those used here. The ratios ρ and ν are easily calculated from these estimates of density and sound speed values at the interfaces.

The loss tangent, δ, is related to the complex sediment acoustic wavenumber $k_2 = k_{2r} + k_{2i}$ and is also related to the attenuation coefficient, α_2, which is usually expressed in dB/m and is discussed in *Hamilton* [1972]. In this study, the results of *Hamilton* [1980] are used to determine values for $\frac{\alpha_2}{f}$ which are based on sediment grain size .

Values for the correlation length, d, of Eq. (41) were obtained by autocorrelation calculations for the depth series of density values from ground truth cores. Density was chosen for the autocorrelation because it exhibited a stronger variation with depth. Figure 12 and Figure 13 show values of the autocorrelation versus lag for the density profiles of two Fingers Area cores. Also shown on these plots is an exponential curve fit to the autocorrelation data. The correlation length is taken to be the point where the autocorrelation function (curve fit) falls to $1/e$ of its original value. Figures 12 and 13 also justify the choice of an exponential representation of the autocorrelation function. Variance of compressibility, cv, was calculated using Eq. (5) with the values of density and compressibility obtained from the ground truth core data.

The spectral exponent, γ, was assigned a value of 3.25. This was done for three reasons: (1) *Briggs* [1989] and *Jackson et al.* [1986b] have found that values of this parameter are usually between 3 and 3.5 with an average of 3.23, (2) the model simulations show almost no dependence of backscattering strength on variation of γ within this range, (3) there are no estimates of roughness in or near the Fingers Area. Values for the spectral strength, β, are estimated with a grain size regression relation developed in *Mourad and Jackson* [1989].

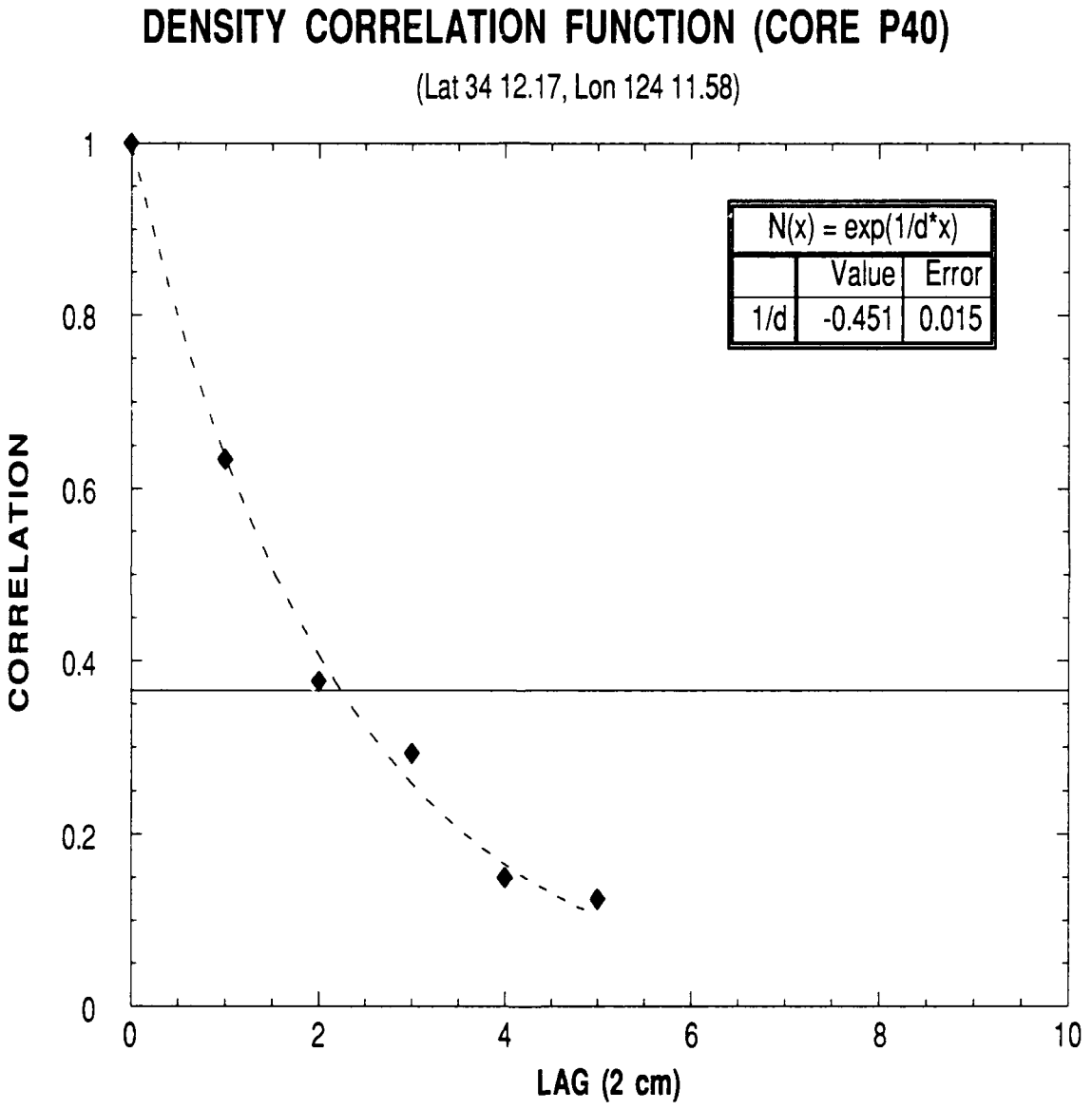

Figure 12. Graph of density correlation function core P40.

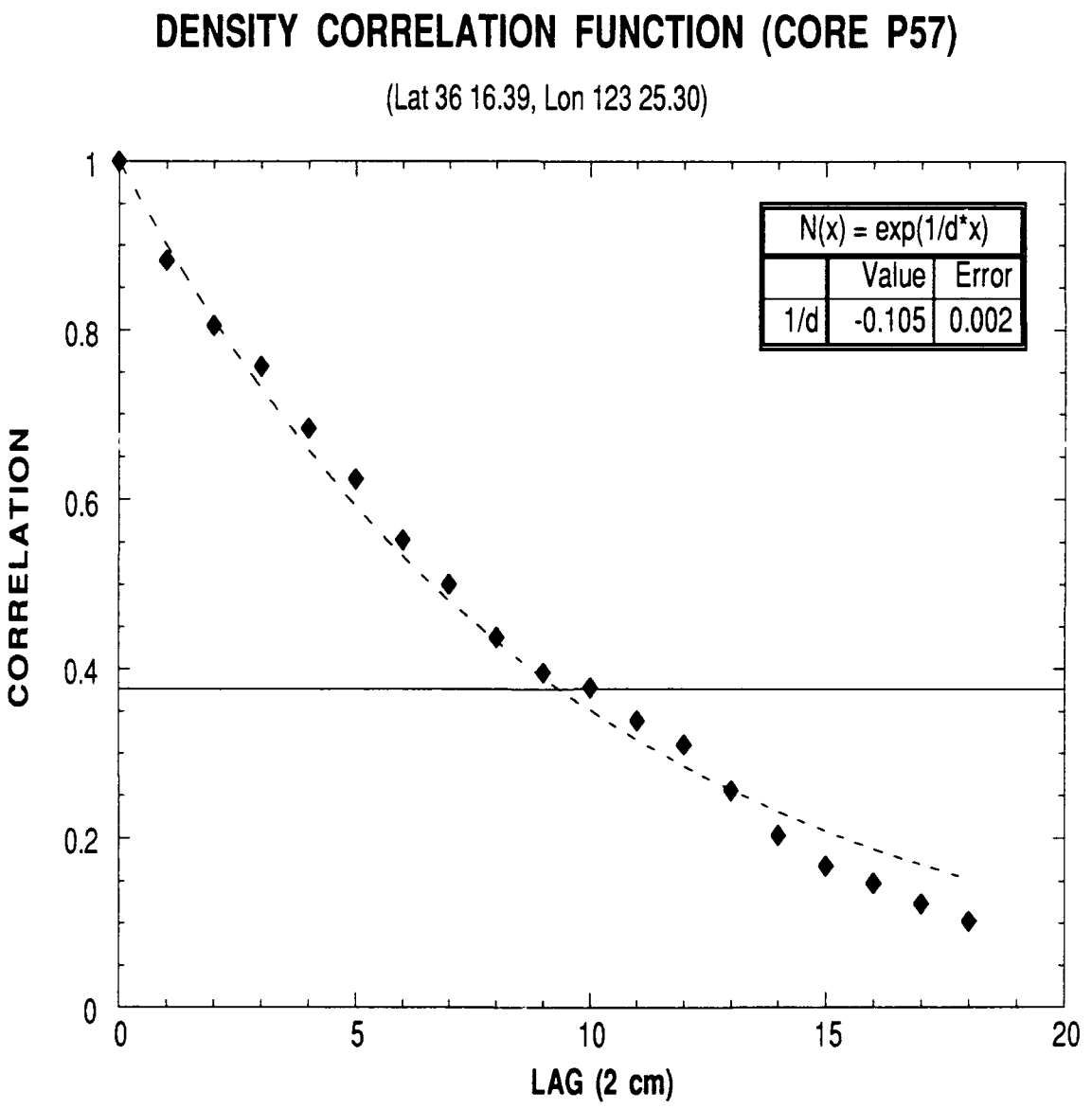

Figure 13. Graph of density correlation function core P57.

Table 1 provides a brief description of the geoacoustic input parameters for the backscattering model with brief remarks about the method for their estimation. Table 2 gives the parameter values used in the model simulations of this study obtained as discussed above.

Table 1. Bottom parameters used as model inputs.

BOTTOM PARAMETERS USED AS MODEL INPUTS

SYMBOL	DEFINITION
ρ	Ratio of sediment mass density to water mass density: this can be obtained from cores and bottom water information.
v	Ratio of sediment sound speed to water sound speed: this can be obtained from cores and bottom water information.
δ	Ratio of imaginary wavenumber to real wavenumber for the sediment: this is a measure of the attenuation in the sediment and can be estimated by knowing the frequency and the attenuation coefficient (which can be estimated from grain size.)
d	Correlation length: this parameter along with the variance of density and compressibility is used to describe the sediment volume and is estimated by running an autocorrelation on the density or compressibility within a core.
cv	Variance of density and compressibility: this parameter along with the correlation length is used to describe the sediment volume and is estimated with the use of core data.
γ	Exponent of bottom relief spectrum: this parameter along with the strength of the bottom relief spectrum is used to describe the random roughness spectrum of the seafloor and is assigned a value of 3.25 for simulation runs.
β	Strength of bottom relief spectrum (cm^4) at wavenumber $2\pi/\lambda = 1\ cm^{-1}$: this parameter along with the spectral exponent is used to describe the random roughness spectrum of the seafloor and is estimated with a regression relation based on grain size.

Table 2. Preset parameters for simulations.

PRESET PARAMETERS FOR SIMULATIONS

sediment-water interface:

ρ = **1.46**
ν = **0.998**
δ = **0.00475**
γ = **3.25**
β = **0.0005175**

first volume:

d = **0.04** m
CV = **0.0087**

subbottom interface:

ρ = **1.24**
ν = **1.28**
δ = **0.01404**
γ = **3.25**
β = **0.0030101**

second volume:

d = **0.01**
CV = **0.0056**

RESULTS, DISCUSSION AND CONCLUSIONS

Introduction

An initial step in carrying out this research project was computer implemention of an existing model of seafloor backscattering [*Jackson et al.*, 1986a]. Two objectives of the research were to use this model (1) to assess, by simulation, the role of different mechanisms (*e.g.* rough interface scattering and volume scattering) in generating seafloor backscattering as observed by long-range side-scan sonar systems and (2) to assess the relative importance of the controlling seafloor geoacoustic parameters to the observed seafloor backscattering strength and its grazing angle dependence.

The complete bottom backscattering strength model used in the simulations consists of two interface scattering terms and two volume scattering terms. Although other scattering components may be present, the ones used here have explained significant aspects of observed backscattering. Also, these are the principal scattering components that could be estimated with model inputs determined from the core descriptions for ground truth data from the acoustically measured region. The simulation input parameters are those described in Table 1. The model results are compared here with GLORIA backscatter data from the Fingers Area. Both the model simulations and the GLORIA inversion results are presented as scattering strength in dB versus grazing angle in degrees.

Comparison of Model Results with GLORIA Inversion Data

In Figure 14, the model predictions obtained using the core constrained input parameter values and a first subbottom layer thickness (depth to first interface) of 130 *cm* are compared to five lines of GLORIA inversion data from the Fingers Area. This subseafloor layer thickness was chosen from information for core P40 (Figure 2). Separate representations of each of the component backscattering cross sections are shown to provide insight into the relative importance of each (remember that the total is obtained by summing intensities, *i.e.* in the linear domain not the logarithmic domain). This combination of input parameter values, based on core P40 provides a reasonable fit of model results to the high return portion of the data. Figure 14 indicates that the high return region is dominated by scattering from the random inhomogeneous continuum within the first subbottom layer, and that returns from the buried sand layer interface are relatively unimportant.

The sensitivity of these model results to initial layer thickness was examined. The model predictions shown in Figure 15 are based on the same input parameter values as Figure 14, but with a first volume thickness of 10 *cm* (slant thickness will be greater as the grazing angle decreases). Core data indicate that, within the low return region the thickness of the topmost silt-clay layer varies between 0 and 10 *cm*. The interface (which is buried for thicknesses greater than zero) dominates the backscattering at high grazing angles while, for the 10 *cm* layer thickness, the volume dominates at lower grazing angles ($< 15°$) where the acoustic energy follows

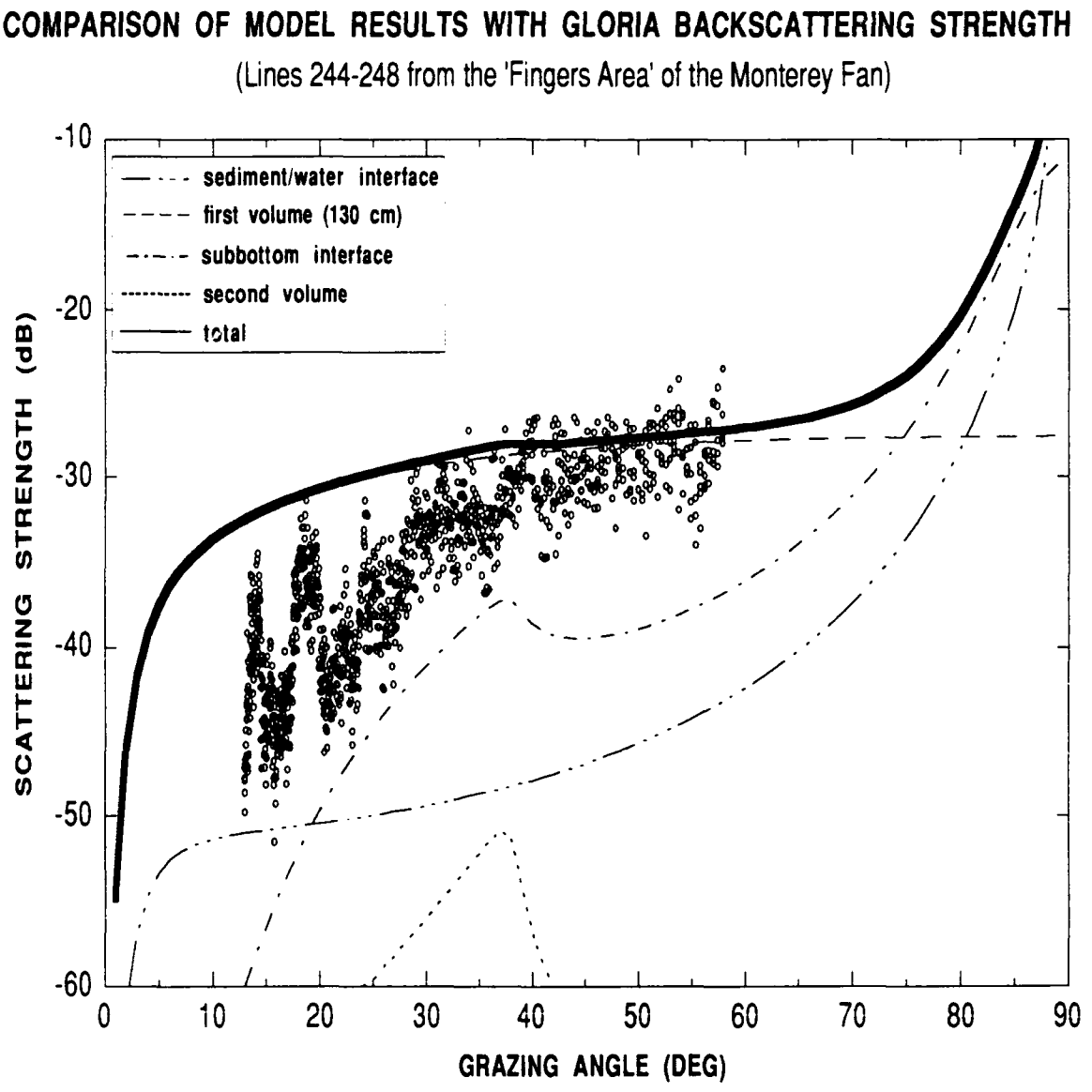

Figure 14. Model simulation with parameters obtained from cores and a 130 *cm* top layer.

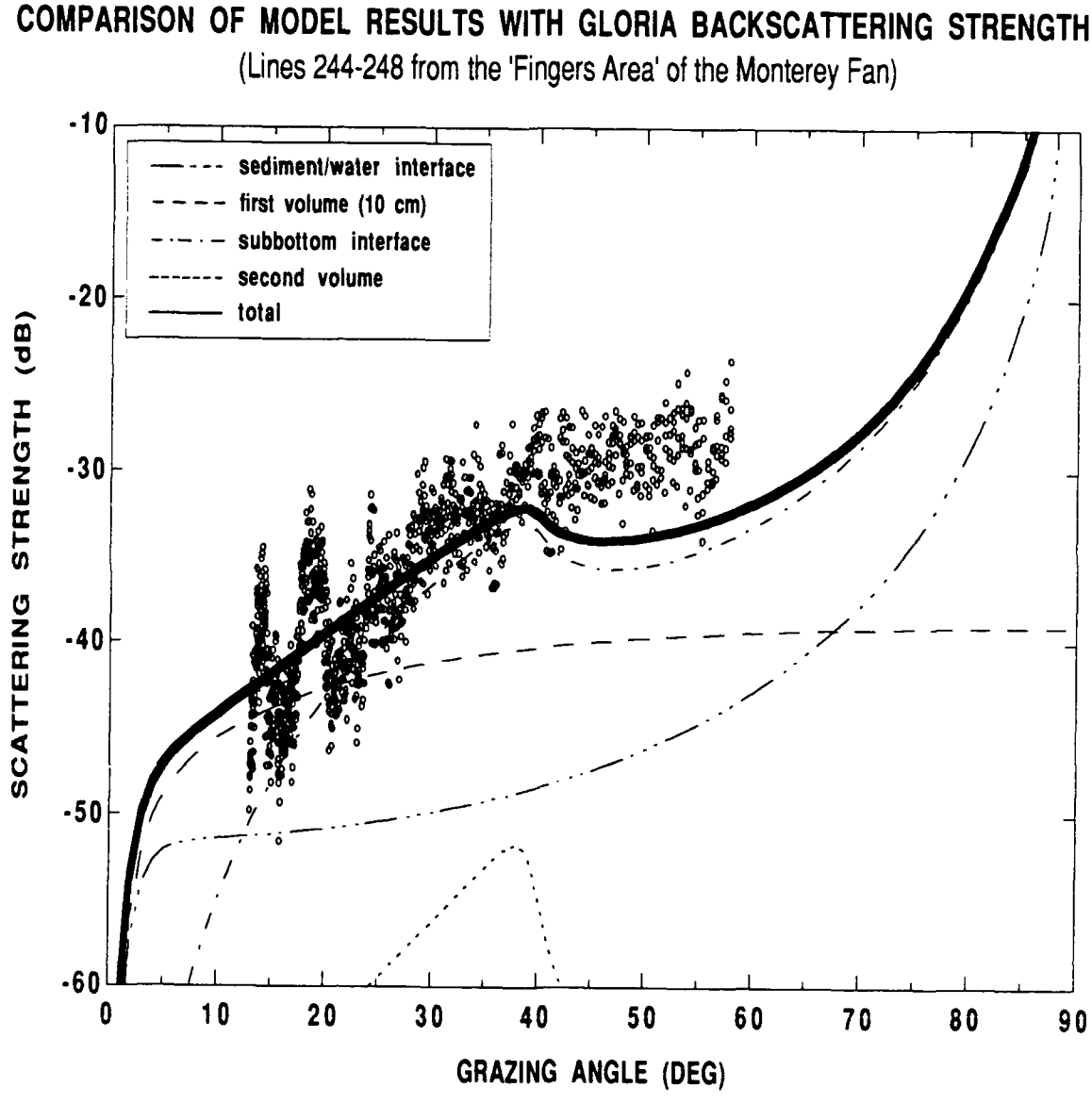

Figure 15. Model simulation with 10 *cm* top layer.

a longer, slanted path through the layer and thus "sees" a thicker volume. The 10 *cm* model layer thickness predictions place an upper bound on the low return "cloud" of values seen in the GLORIA inversion data. The bottom of this low return cloud of values in the data is matched by model results obtained with the topmost sediment layer completely removed, as shown in Figure 16. The seafloor backscattering with no topmost layer volume scattering is dominated by interface scattering at the top of the sand layer. This interface is a fairly strong scatterer for three reasons: the impedance mismatch is large, the spectral strength of the sand interface is large and there is a peak in the scattering strength near the critical angle for this interface.

Figures 14, 15, and 16 show that, even with the limited number of good ground truth cores available for the study area to estimate model input parameters, the fit of model results to experimental data is reasonable over the span of grazing angles from 13° to 43°. Additional strongly scattering interfaces, which are not included in these predictions may contribute to the discrepency between 45°-55°. The effect of such additional interfaces would be greater at these higher angles because of shorter subseafloor ray paths and thus decrease in attenuation. The results in these three figures also suggest that the seafloor parameter values estimated from the ground truth cores are representative of the average values for the entire Fingers Area. Variations in scattering strength which are shown in later figures probably result from horizontal variations in parameter values.

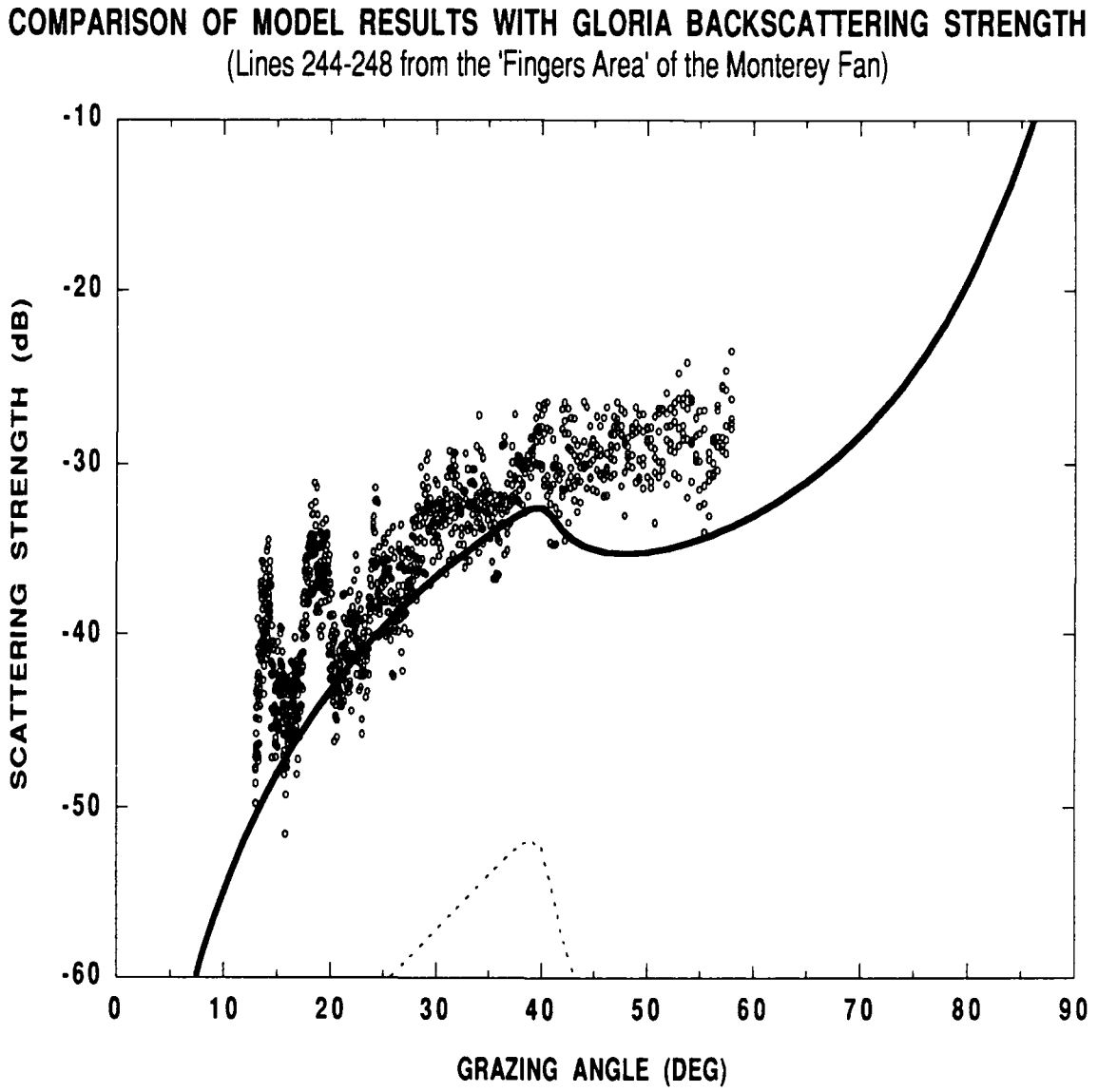

Figure 16. Model simulation with no top layer.

Sensitivity Tests

Sensitivity tests were run to develop a better understanding of the relationships between the controlling geoacoustic parameters and the acoustic backscattering, in terms of both the level and the grazing angle dependence of seafloor backscattering strength. The results of such tests for several of the more important parameters are shown in Figures 17-23.

Figure 17 shows the effect of first (topmost) layer thickness on predictions of backscattering strength versus grazing angle. The main control on the difference between the two scattering regimes shown in Figures 14-16, the top layer thickness, is evident on Figure 17. The volume scattering component increases as the scattering volume increases. At greater layer thickness, the scattering from the first inhomogeneous continuum dominates the subbottom interface scattering. This results from both the increased scattering volume of the layer and the increased attenuation along the longer paths in the layer (to the buried scattering interface).

The relationship between correlation length of the volume inhomogeneities and the backscattering strength versus grazing angle is shown in Figure 18. Changes in the value of the correlation length produce changes in the grazing angle dependence of backscattering. This relationship results from the combined effects of the strong dependence of scattering cross section per unit volume on the correlation length (Figure 9) and the increase of correlation length with decreasing grazing angles due to anisotropy. The results of these combined effects are apparent at the low grazing angles shown in Figure 18.

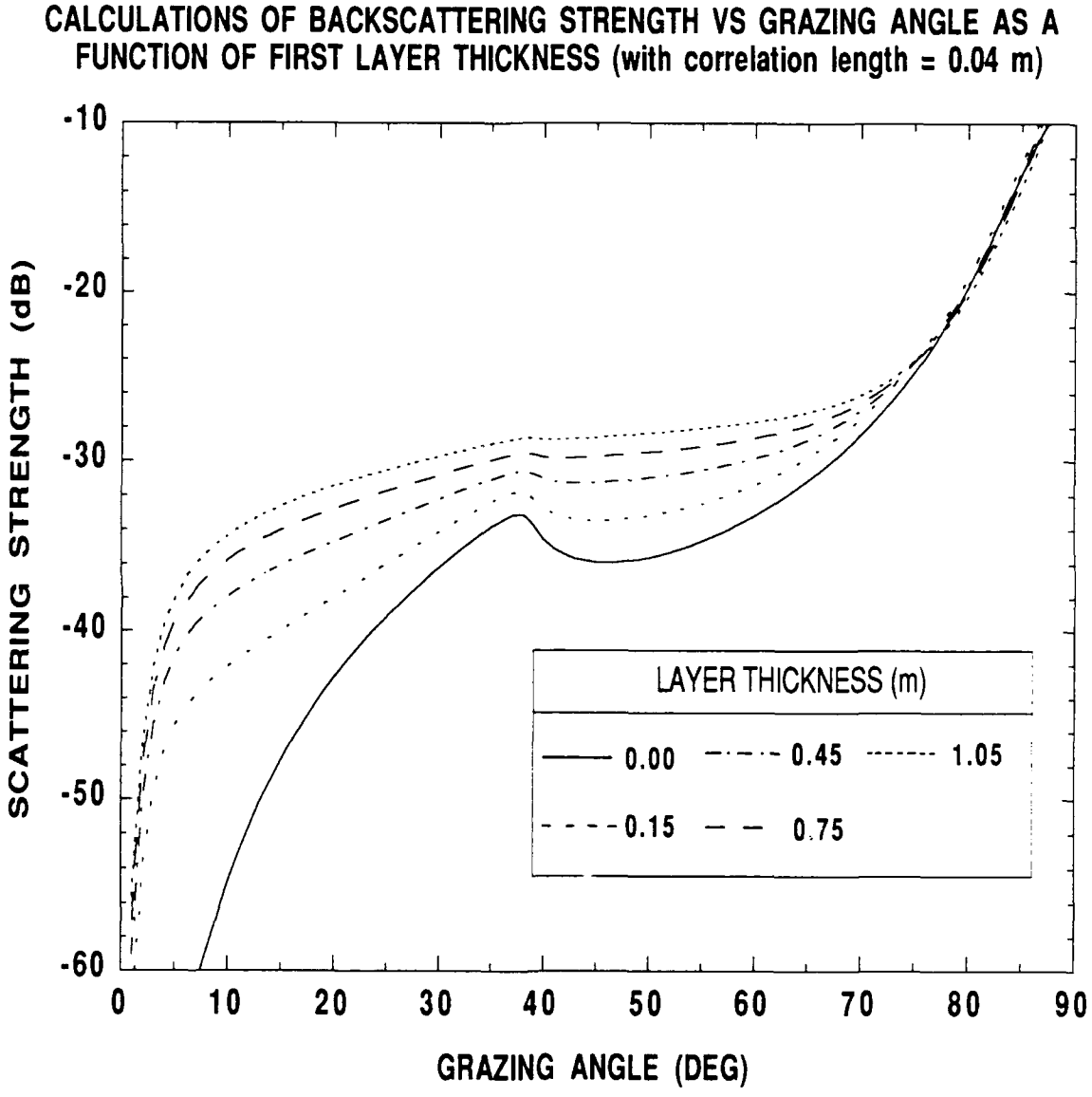

Figure 17. Layer thickness dependence of backscatter.

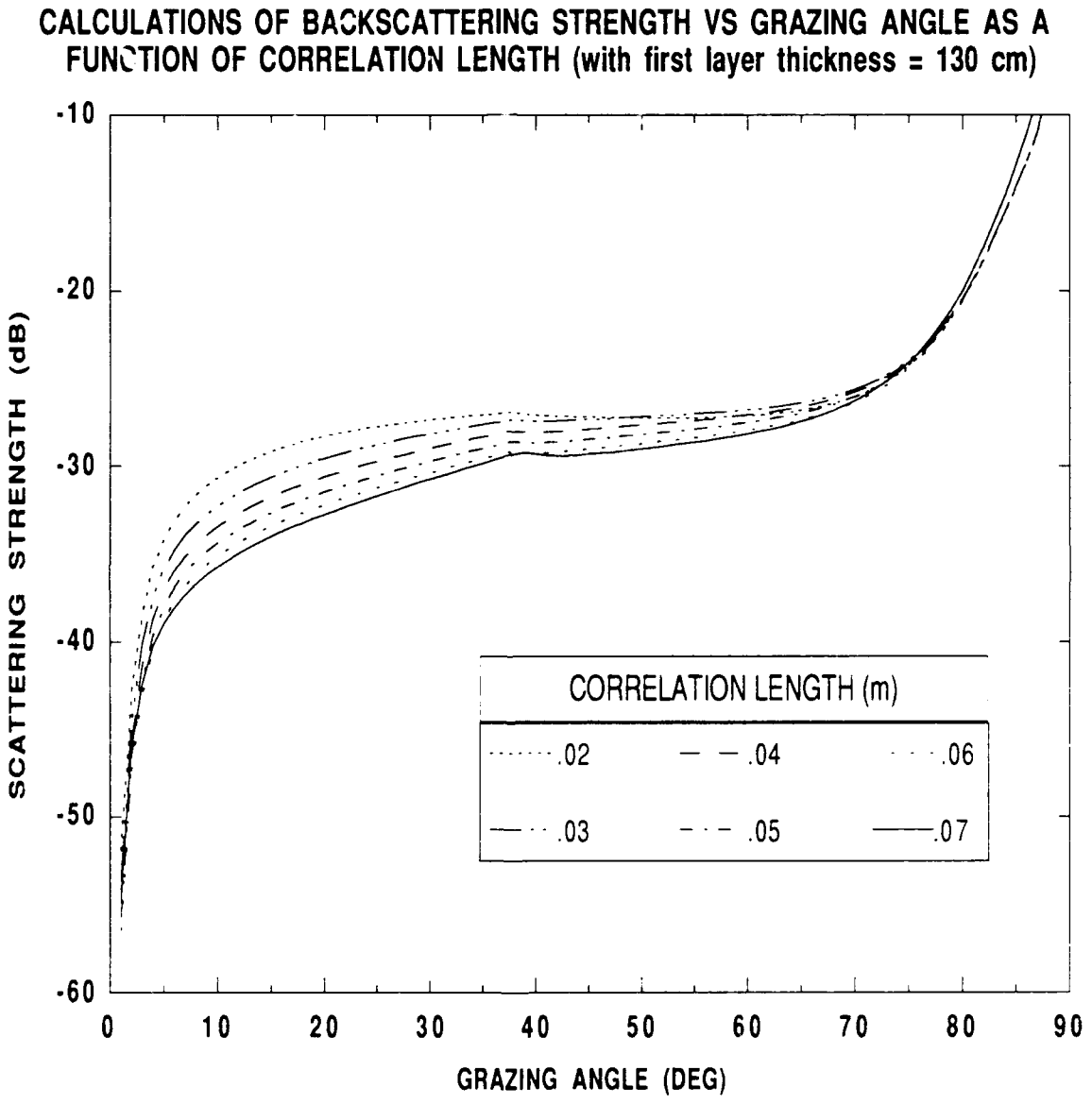

Figure 18. Correlation length dependence of backscatter.

With model input parameter values constrained by Fingers Area ground truth measurements, only weak frequency dependence of backscatter is predicted with maximum dependence exhibited for seafloor grazing angles near values for the subbottom interface critical angle (Figure 19). This result might appear to be at variance with the strong frequency dependence of scattering cross section shown in Figure 10 for correlation lengths near the 4 *cm* correlation length used in the simulations. However, the effect of anisotropy is to increase the effective correlation length thus reducing the frequency dependence (reference Figure 10). The primary frequency dependence is the scattering from the subbottom interface which is especially evident near the critical angle for this interface.

Using various values of density and velocity ratio as given in *Jackson et al.* [1986a], provides the model simulations, with no volume scattering, which are presented in Figure 20. These results show the effect, on the interface backscattering strength, of increasing the acoustical "hardness" of the interface. The greater impedance contrast across the interface increases the scattering strength. It can also be noted that increasing values of seafloor velocity cause an increase of scattering near the critical angle (a result of the Rayleigh-Rice approximation).

Spectral strength of interface roughness has a very strong effect on the scattering strength of the subbottom interface (Figure 21). The range of values used in the predictions for Figure 21 is wider than the range estimated from grain size data for the ground truth cores (0.0005-0.003). The highest values of the spectral strength used for the predictions of Figure 21 would only occur in regions where the bottom is extremely rough.

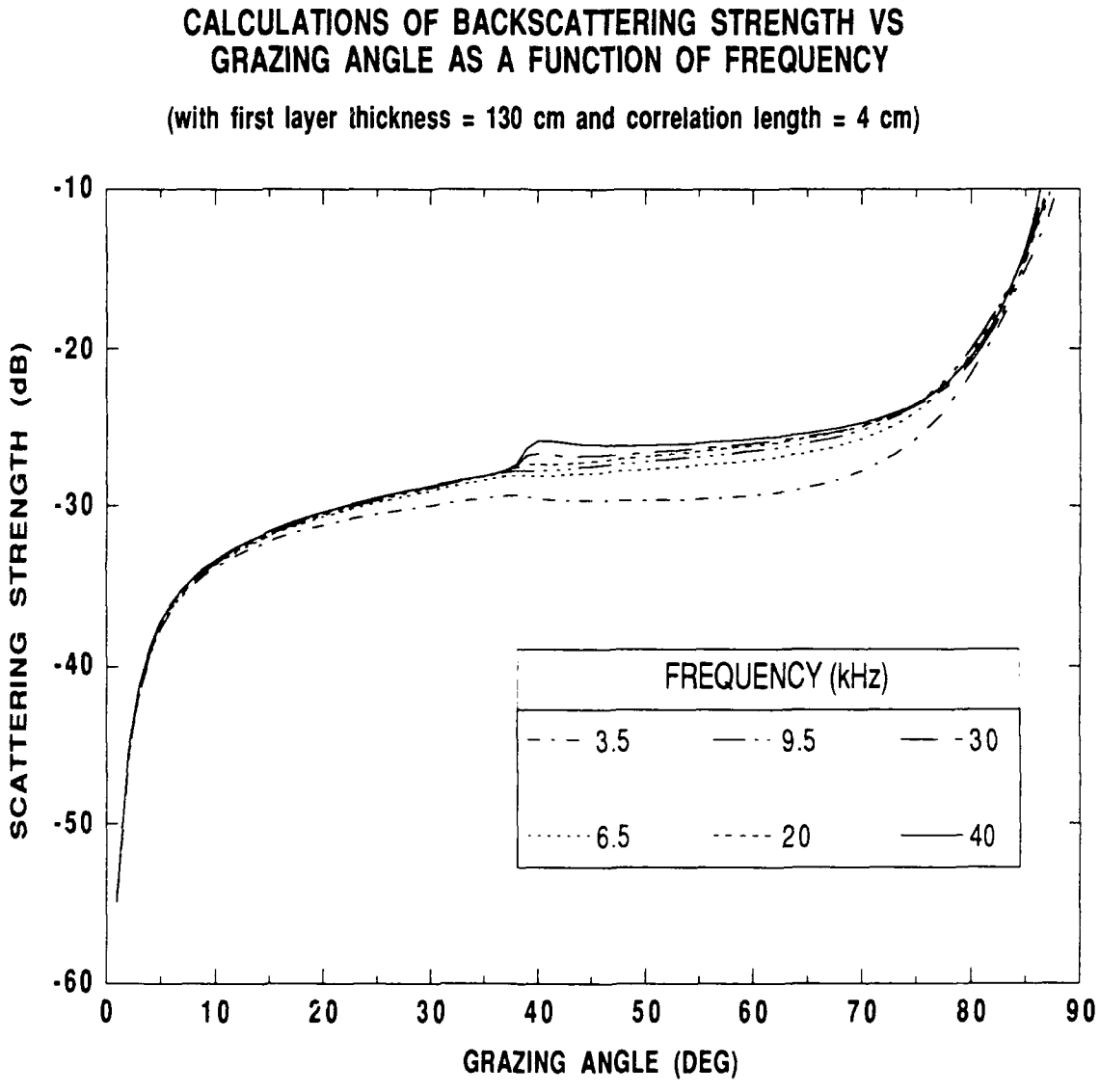

Figure 19. Frequency dependence of backscatter.

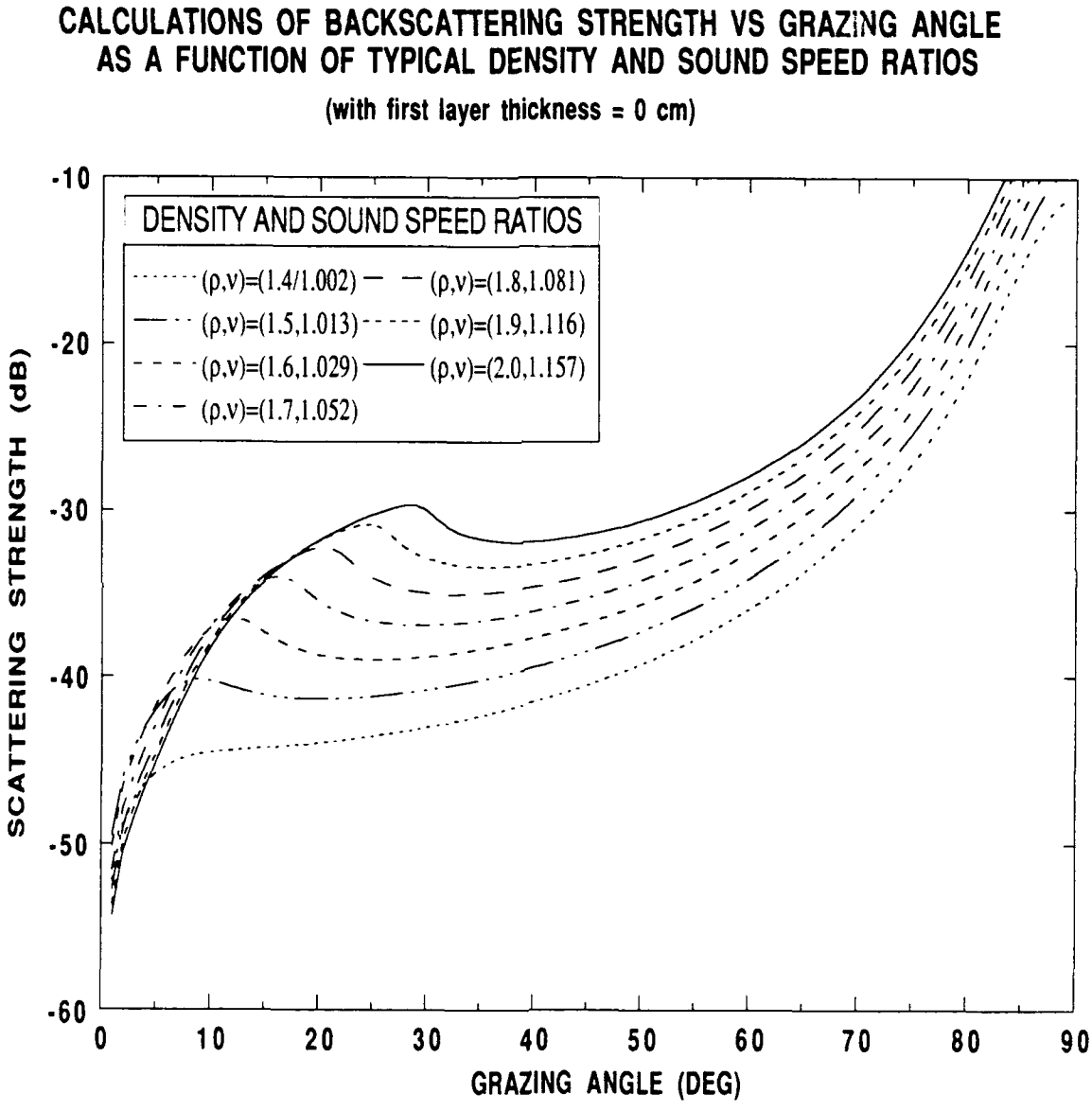

Figure 20. Density and sound speed ratio dependence of backscatter.

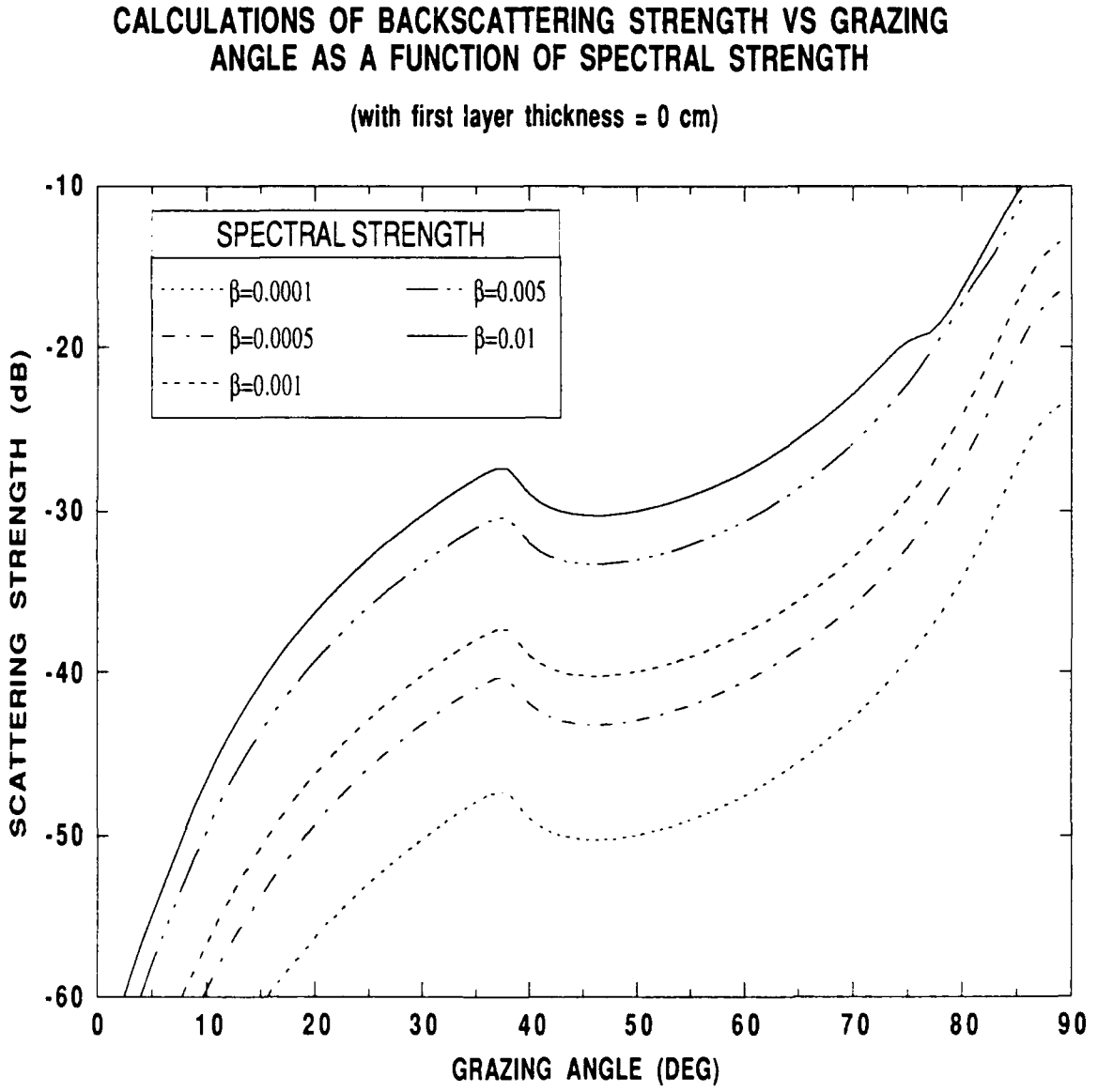

Figure 21. Spectral strength dependence of backscatter.

Figure 22 provides simulation results for conditions which are the same as those used to generate Figure 18 but with the correlation length reduced even further to 1 *cm*. The scattering cross section per unit volume (Figure 9) now moves from the left side of the peak to the right side as grazing angle is decreased (with consequent increase of effective correlation length due to anisotropy). This has the effect of increasing scattering strength at lower grazing angles which is seen on Figure 22. It is interesting that similar grazing angle dependence can be seen in Figure 8.28 in *Urick* [1983] suggesting the existence of smaller correlation lengths for the subseafloor inhomogeneities in the region of the measurements Urick reports.

If the correlation function of the inhomogeneous continuum is Gaussian instead of exponential so that

$$N(x) = exp(-x^2/d^2), \tag{45}$$

then the scattering cross section per unit volume changes from Eq. (41) to

$$\mu = \frac{k^4 d^3}{16\sqrt{\pi}} \left(\frac{\sqrt{\langle |\Delta\kappa|^2 \rangle}}{\kappa_0} + \frac{\sqrt{\langle |\Delta\rho|^2 \rangle}}{\rho_0} \right)^2 exp[-k^2 d^2]. \tag{46}$$

The shape of a graph of the scattering cross section per unit volume versus correlation length becomes very peaked, falling to zero on both sides of the peak. Figure 23 shows the effect of a Gaussian correlation function on seafloor scattering strength versus grazing angle . Two plateaus are evident on the figure. It is not known if this behavior has been seen in backscattering data.

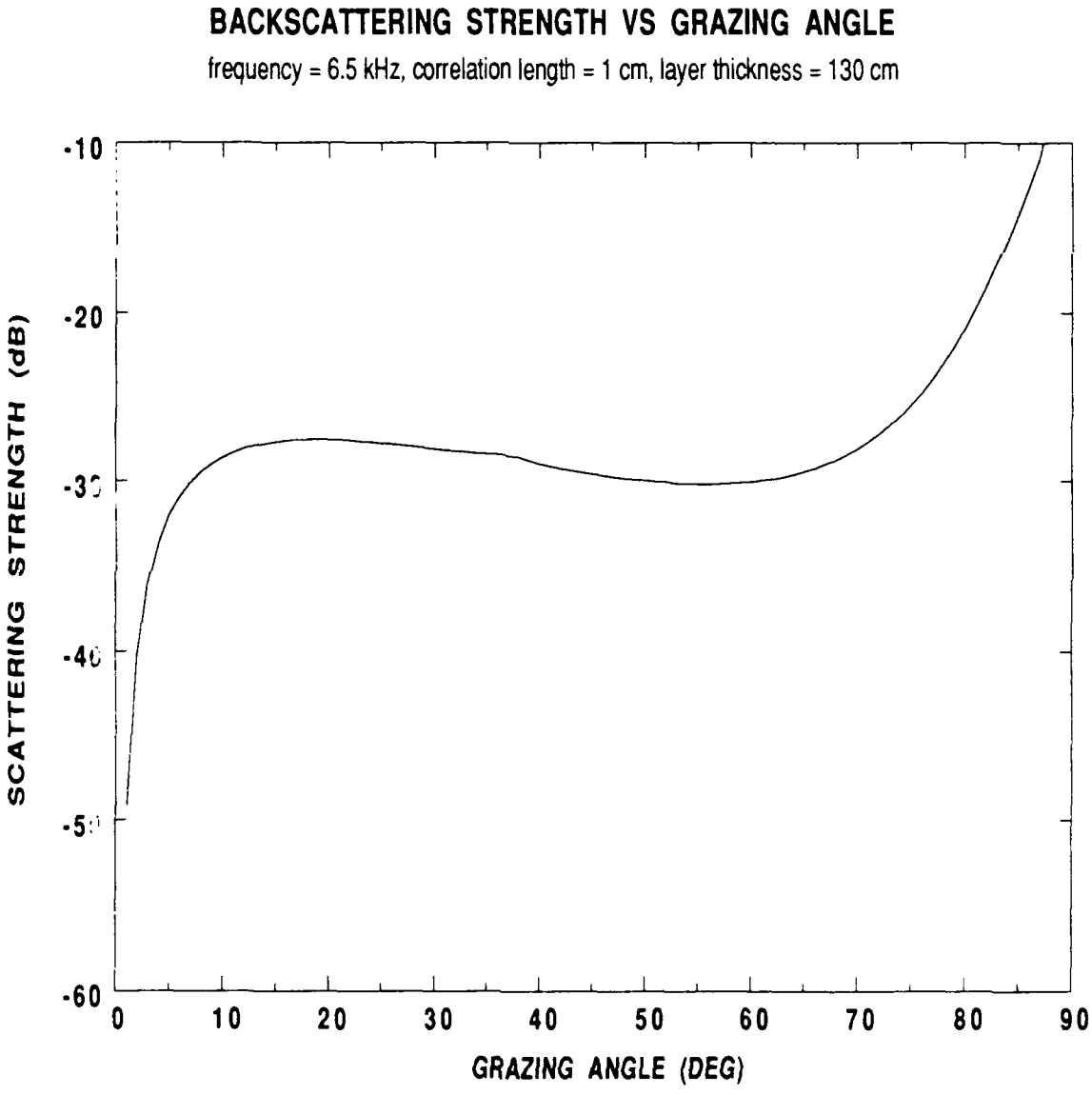

Figure 22. Effect of changing correlation length on backscatter.

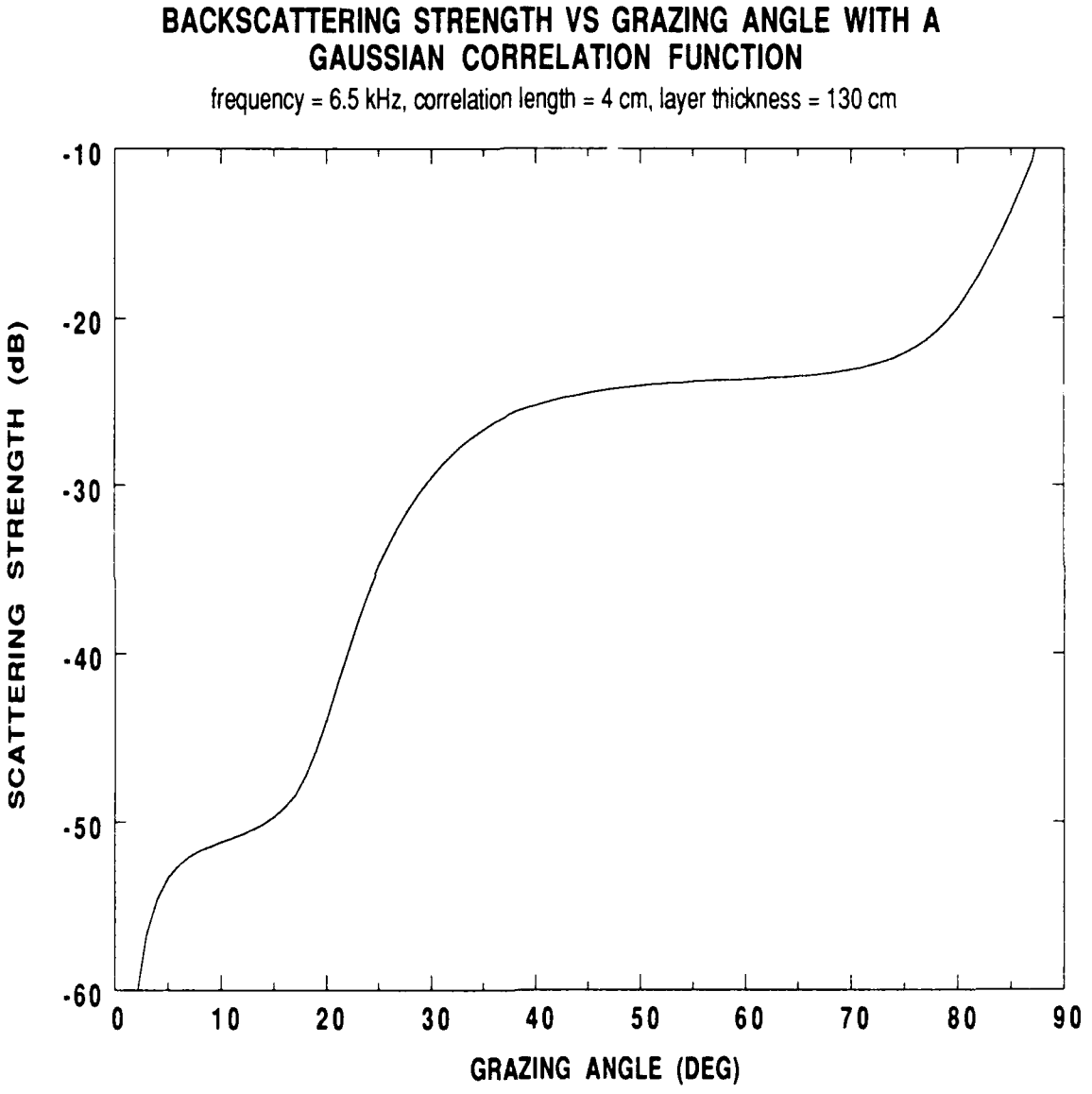

Figure 23. Effect of using a gaussian correlation function on backscatter.

The results of sensitivity studies, as illustrated above, have resulted in greater understanding of the relationship between the level and grazing angle dependence of seafloor backscattering and the seafloor geoacoustic parameters of correlation length and top layer thickness. This understanding allows adjustment of the input values for these two parameters in order to generate simulations of backscattering which better fit the inversion data. The final "best fit" model input parameter values may represent better estimates of the study area averages of correlation length and layer thickness. The ground truth cores only provide point estimates of these parameters which are a single member of the ensemble of parameter values for the nearby seafloor. Figures 24-26 show comparisons of new simulation results with groups of eight GLORIA inversion data lines in different parts of the Fingers Area. For these new simulations, *the correlation length was increased to 6 cm and the top layer thickness was reduced* to 110 *cm*. These results indicate how horizontal changes in geoacoustic parameter values can affect the shape of scattering strength versus grazing angle curves.

Conclusions and Recommendations

The model of *Jackson et al.* [1986a], with the additions of scattering from sub-bottom interfaces and scattering from random inhomogeneous continuums, appears to adequately describe backscattering strength versus grazing angle at the GLORIA system frequency. Simulations with the extended model were compared with inverted GLORIA data from the Fingers Area of the Monterey Fan. Input parameter values for the simulations were determined by independent ground truth core data. The

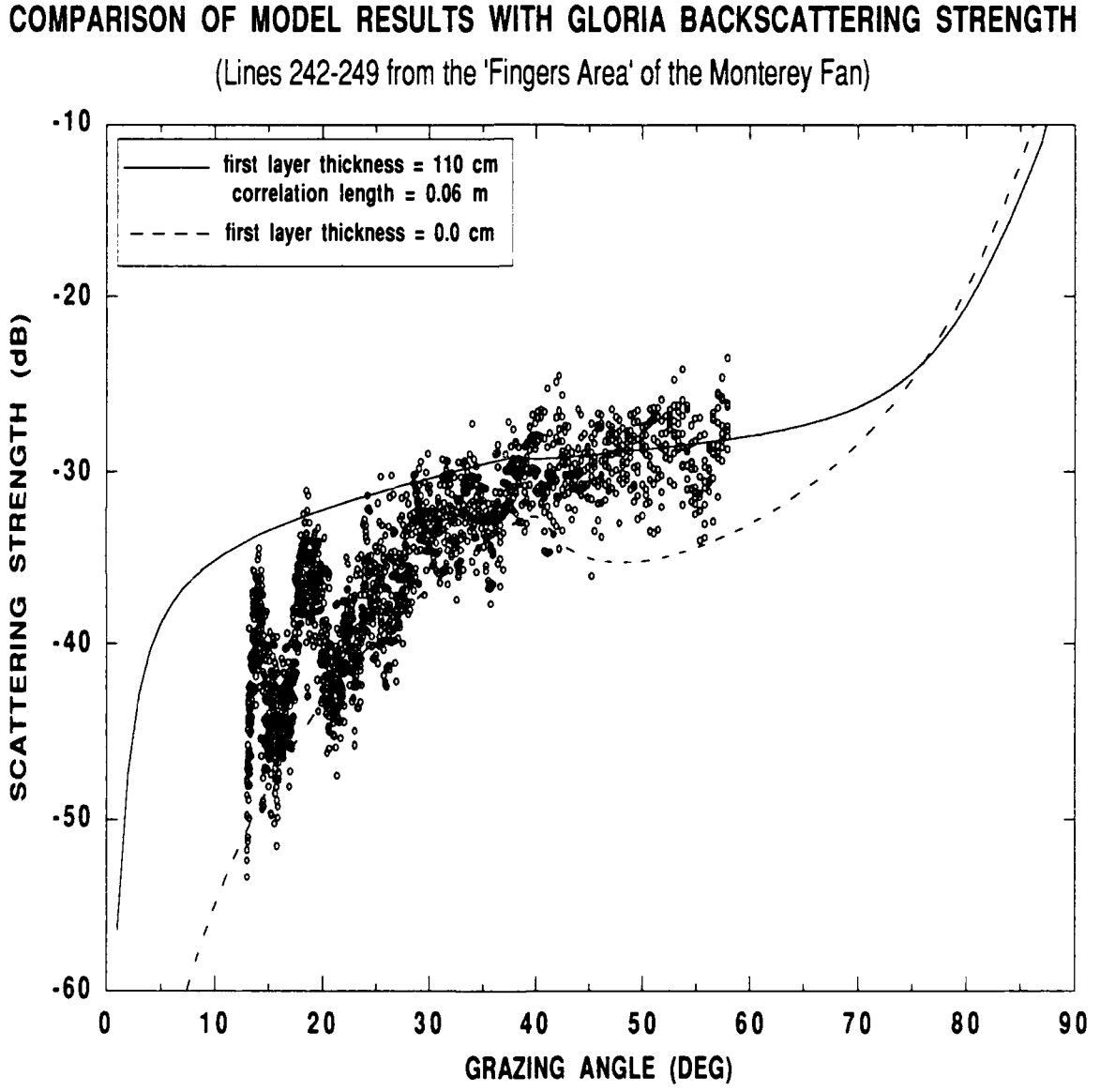

Figure 24. Comparison of data with simulation after changing parameters slightly.

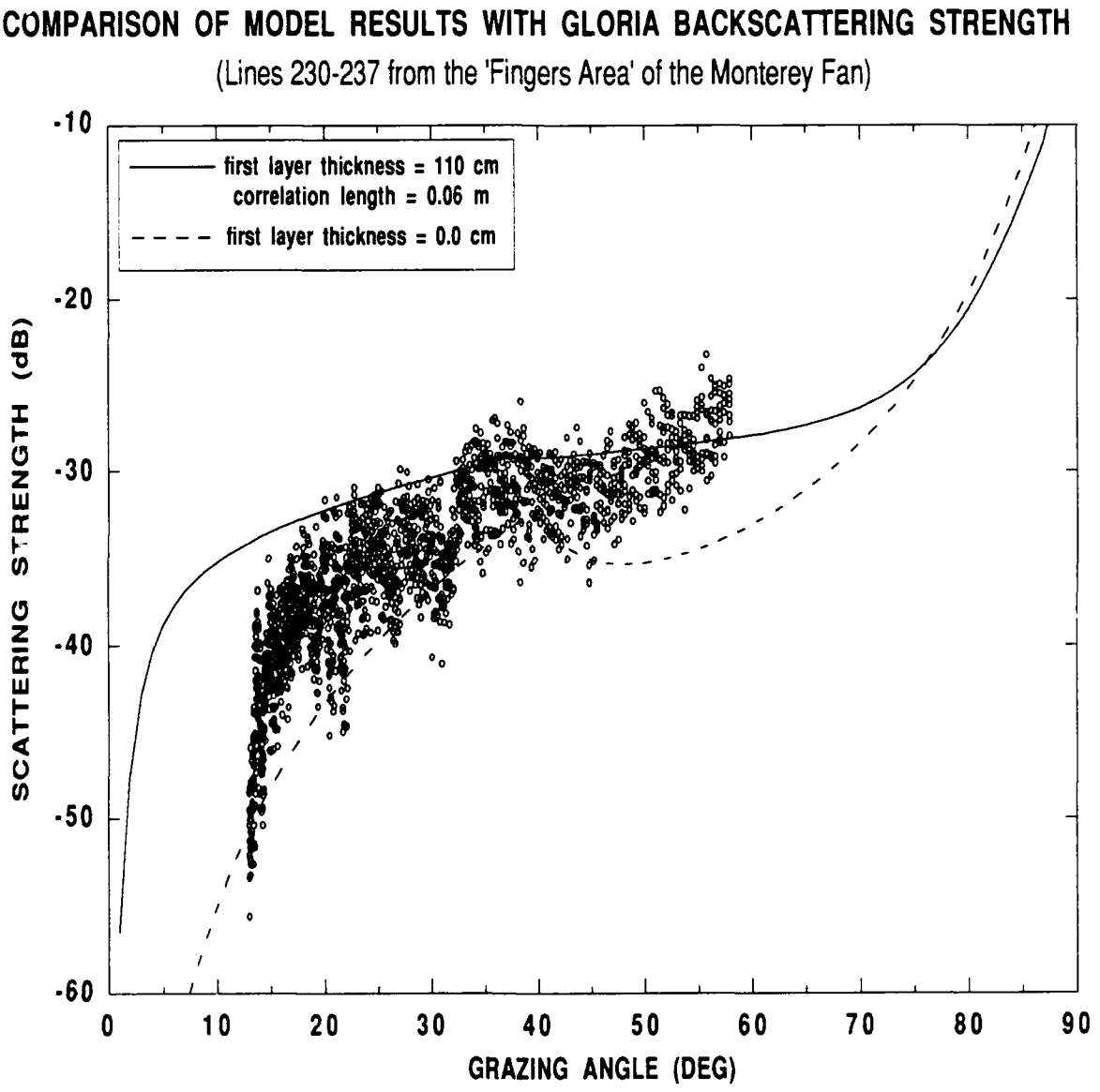

Figure 25. Same as Figure 24 compared with lines 230-237.

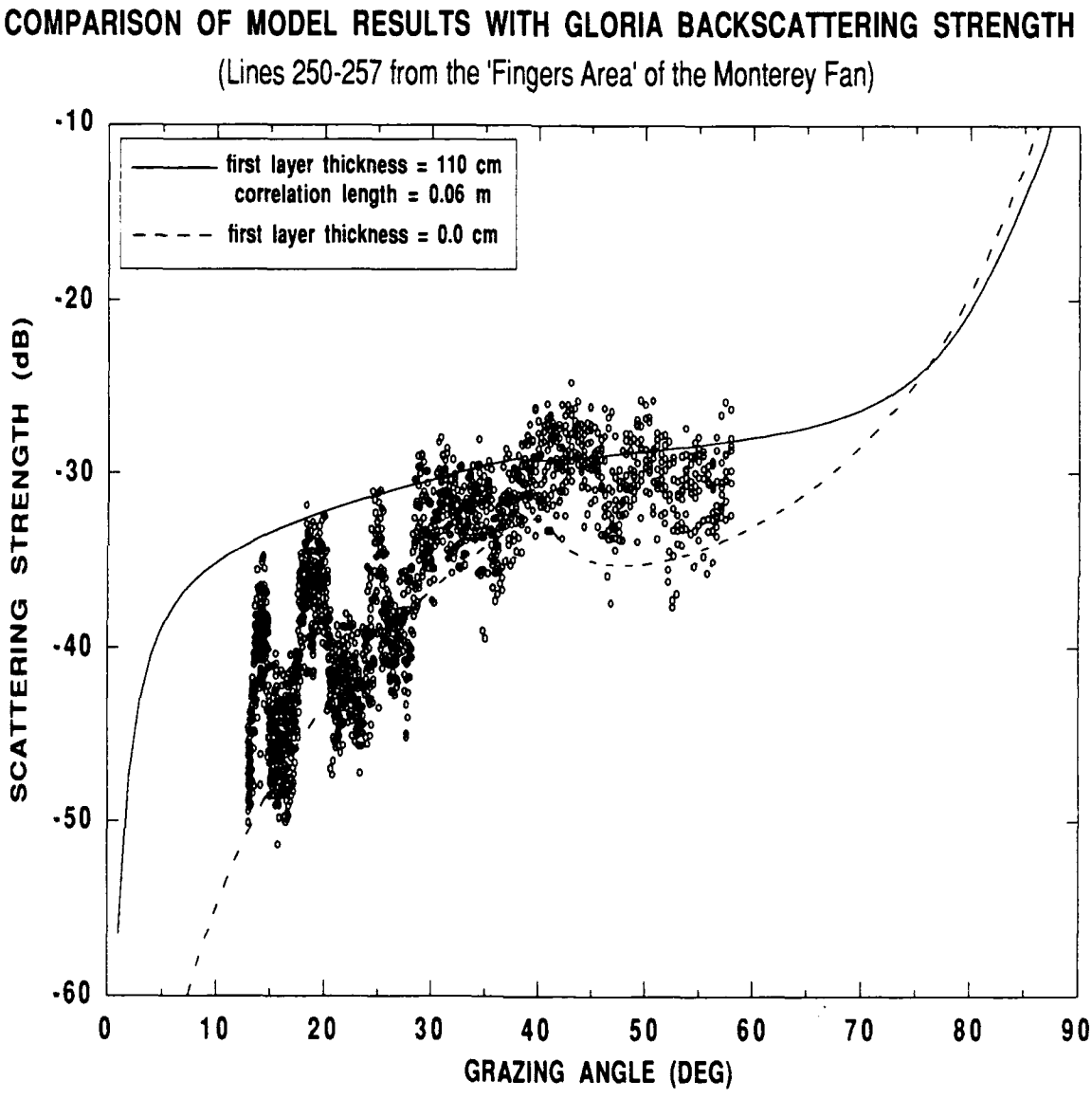

Figure 26. Same as Figure 24 compared with lines 250-257.

results of the comparison support the validity of the final model and increase the understanding of geoacoustic controls on and the physical mechanisms of bottom backscattering. The main factor causing ths observed dichotomous character of the strength of returns in the Fingers Area appears to be the thickness of the first inhomogenous scattering layer, with inhomogeneous volume scattering dominating the high backscatter strength areas and an acoustically hard, shallow subbottom interface dominating the low backscatter strength areas. The upper one and one-half meters of sediment seem to be controlling the observed scattering strength values in the Fingers Area.

Several items must bc addressed to further test the validity of the resulting extended model. More ground truth cores are needed than were used in this study. Since the cores give only point estimates of the parameter values used in the model, the parameters are probably not true averages for the study area - although the results indicate that the values used must approximate the true averages. More cores could provide estimates of the horizontal changes in parameter values that could be used in comparisons to examine the variation of backscattering strength within and between the two identified backscattering regimes. The least confident parameter estimates are those for the interface roughness. The spectral exponent value is probably reasonable because of the narrow range of values for this parameter found in this type of sediment environment. Because of the strong influence of the spectral strength of the roughness on seafloor backscattering strength, the roughness parameter should be measured for the Fingers Area.

There are a few experiments that might be useful to test the model. A multifrequency measurement of backscattering strength from a seafloor "patch" could test the possibility of using backscattering strength values at different frequencies as an indicator of a dominant correlation length for the volume inhomogeneities. A study in an area where the correlation lengths are isotropic (such as a heavily bioturbated area) could examine the effect of degree of anisotropy on the grazing angle dependence of backscattering. A repeat of the present study in a different location, incorporating the recommendations made above, would probably be the best test of the validity of the backscattering model developed for this thesis.

REFERENCES

Briggs, K.B., Microtopographical roughness of shallow-water continental shelves, *IEEE J. Oceanic Engineering, 14*, 360-367, 1989.

Boehme, H., and N.P. Chotiros, Acoustic backscattering at low grazing angles from the ocean bottom, *J. Acoust. Soc. Am., 84*, 1018-1029, 1988.

Chavez, P.S., Jr., Processing techniques for digital sonar images from GLORIA, *Photogrammetric Engineering and Remote Sensing, 52*, 1133-1145, 1986.

Chernov, L.A., *Wave Propagation in Random Medium*, Dover, New York, 1960.

Clay, C.S., and H. Medwin, *Acoustical Oceanography: Principles and Applications*, Wiley Interscience, New York, 1977.

Crowther, P.A., Some statistics of the sea-bed and scattering therefrom, in *Acoustics and the Sea-bed*, edited by N.G. Pace, pp. 147-155, Bath University, Bath, 1983.

Dwan, F.S., Acoustic facies analysis of side-scan sonar data, dissertation, Texas A&M University, 1991.

Felsen, L.B., Quasi-optic diffraction, in *Proceedings of the Symposium on Quasi-optics*, edited by J. Fox, pp. 1-40, John Wiley and Sons, New York, 1964.

Fox, C.G., and D.E. Hayes, Quantitative methods for analyzing the roughness of the seafloor, *Rev. Geophys., 23*, 1-48, 1985.

Gardner, J.V., M.E. Field, H. Lee, B.E. Edwards, D.G. Masson, N. Kenyon, and R.B Kidd, Ground-truthing 6.5 kHz side scan sonographs: what are we really imaging?, *J. Geophys. Res., 96*, 5955-5974, 1991.

Hamilton, E.L., Compressional wave attenuation in marine sediments, *Geophysics, 37*, 620-646, 1972.

Hamilton, E.L., Geoacoustic modeling of the seafloor, *J. Acoust. Soc. Am., 68*, 1313-1340, 1980.

Hamilton, E.L.,and R.T. Bachman, Sound velocity and related properties of marine sediments, *J. Acoust. Soc. Am., 72*, 1891-1904, 1982.

Ishimaru, A., *Wave Propagation and Scattering in Random Media*, Academic Press, New York, 1978.

Jackson, D.R., D.P. Winebrenner, and A. Ishimaru, Application of the composite roughness model to high-frequency bottom backscattering, *J. Acoust. Soc. Am.*, *79*, 1410-1422, 1986a.

Jackson, D.R., A.M. Baird, J.J. Crisp, and P.A.G. Thomson, High-frequency bottom backscatter measurements in shallow water, *J. Acoust. Soc. Am.*, *80*, 1188-1199, 1986b.

Johnson, H.P., and M. Helferty, The geological interpretation of side-scan sonar, *Rev. Geophys.*, *28*, 357-380, 1990.

Kuo, E.Y., Wave scattering and transmission at irregular surfaces, *J. Acoust. Soc. Am.*, *36*, 2135-2142, 1964.

McDaniel, S.T., and A.D. Gorman, Acoustic and radar sea surface backscatter, *J. Geophys. Res.*, *87*, 4127-4136, 1982.

McDaniel, S.T., and A.D. Gorman, An examination of the composite-roughness scattering model, *J. Acoust. Soc. Am.*, *73*, 1476-1486, 1983.

Mitchell, N.C., and M.L. Somers, Quantitative backscatter measurements with a long-range side-scan sonar, *IEEE J. Ocean. Eng.*, *14*, 368-374, 1989.

Mourad, P.D., and D.R. Jackson, High frequency sonar equation models for bottom backscatter and forward loss, in *Oceans '89 Proceedings*, pp. 1168-1175, IEEE, New York, 1989.

Nassiri, D.K., and C.R. Hill, The use of angular acoustic scattering measurements to estimate structural parameters of human and animal tissues, *J. Acoust. Soc. Am.*, *79*, 2048-2054, 1986.

Nicholas, D., Ultrasonic scattering and structure of human tissue, Ph.D. Thesis, University of London, 1976.

Nolle, A.W., W.A. Hoyer, J.F. Mifsud, W.R. Runyan, and M.B. Ward, Acoustical properties of water filled sands, *J. Acoust. Soc. Am.*, *35*, 1394-1408, 1963.

Rayleigh, J.W.S., *Theory of Sound*, Dover, New York, 1945.

Stanton, T.K., Sonar estimates of seafloor microroughness, *J. Acoust. Soc. Am.*, *75*, 809-818, 1984.

Stockhausen, J.H., Scattering from the volume of an inhomogeneous half-space, *Report No. 63/9*, Naval Research Establishment, Canada, 1963.

Stoll, R.D., Marine sediment acoustics, *J. Acoust. Soc. Am.*, *77*, 1789-1799, 1985.

Thorsos, E.I., The validity of the Kirchhoff approximation for rough surface scattering using a Gaussian roughness spectrum, *J. Acoust. Soc. Am.*, *83*, 78-92, 1988.

Thorsos, E.I., and D.R. Jackson, The validity of the perturbation approximation for rough surface scattering using a Gaussian roughness spectrum, *J. Acoust. Soc. Am.*, *86*, 261-277, 1989.

Urick, R.J., *Principles of Underwater Sound*, McGraw-Hill, New York, 1983.

Wagner, R.J., Shadowing of randomly rough surfaces, *J. Acoust. Soc. Am.*, *41*, 138-147, 1967.

Wong, H.K., and W.D. Chesterman, Bottom backscattering near grazing incidence in shallow water, *J. Acoust. Soc. Am.*, *44*, 1713-1718, 1968.

Wyber, R.J., The dependence of bottom backscattering on the structure of a layered scattering medium, *J. Acoust. Soc. Am.*, *78*, 665-671, 1985.

Supplementary Sources Consulted

Dwan, F.S., A.L. Anderson, and J.V. Gardner, Seafloor acoustic facies analysis of side-scan sonar data (abstract), *EOS Trans. AGU*, *70*, 1305, 1989.

Wenzel, A.R., and J.B. Keller, Propagation of acoustic waves in a turbulent medium, *J. Acoust. Soc. Am.*, *50*, 911-920, 1971.